

# Principal component analysis for max-stable distributions

Felix Reinbott,<sup>a,\*</sup> Anja Janßen<sup>a</sup>

<sup>a</sup>*Institute for Mathematical Stochastics, Otto-von-Guericke University Magdeburg*

---

## Abstract

Principal component analysis (PCA) is one of the most popular dimension reduction techniques in statistics and is especially powerful when a multivariate distribution is concentrated near a lower-dimensional subspace. Multivariate extreme value distributions have turned out to provide challenges for the application of PCA since their constraint support impedes the detection of lower-dimensional structures and heavy-tails can imply that second moments do not exist, thereby preventing the application of classical variance-based techniques for PCA. We adapt PCA to max-stable distributions using a regression setting and employ max-linear maps to project the random vector to a lower-dimensional space while preserving max-stability. We also provide a characterization of those distributions which allow for a perfect reconstruction from the lower-dimensional representation. Finally, we demonstrate how an optimal projection matrix can be consistently estimated and show viability in practice with a simulation study and application to a benchmark dataset.

*Keywords:* Dimension reduction, Extreme value statistics, Max-stable distributions, Principal component analysis, Tropical linear algebra.

*2020 MSC:* Primary 62G32, Secondary 62H25

---

## 1. Introduction

Multivariate, potentially high-dimensional data frequently emerges in various applications, and it is of fundamental interest to extract key features and patterns from datasets. For this task, a large variety of unsupervised learning algorithms have been developed and applied to different settings, for a general overview see for example [9] or [34]. One of the most frequently used techniques is principal component analysis (PCA), performing especially well if the data concentrates around a low dimensional linear subspace, see [36] and [42].

One way to motivate PCA is via the representation of multivariate normal distributions. Remember that for a  $d$ -dimensional random variable  $X$  following a multivariate normal distribution with mean  $(0, \dots, 0)$  and covariance matrix  $\Sigma \in \mathbb{R}^{d \times d}$ , there exist an orthogonal matrix  $Q \in \mathbb{R}^{d \times d}$  and a diagonal matrix  $D \in [0, \infty)^{d \times d}$  such that

$$X \stackrel{d}{=} Q \cdot D \cdot Z,$$

where  $Z$  is a  $d$ -dimensional vector of i.i.d. standard normal random variables and  $\stackrel{d}{=}$  stands for equality in distribution. Both  $Q$  and  $D$  can be deduced from the singular value decomposition of  $\Sigma$  and can be chosen in a way such that the diagonal entries of  $D^2$  are the eigenvalues of  $\Sigma$  in descending order. The columns of  $Q$  are called the principal components of  $X$ . Now,  $X$  lives on a lower-dimensional subspace (i.e. its covariance matrix does not have full rank), if and only if some diagonal entries of  $D$  are 0. More precisely, if only  $p < d$  diagonal entries of  $D$  are positive, the random vector  $X$  can be represented with the help of the lower dimensional random vector  $(Z_1, \dots, Z_p)$  consisting of only  $p$  i.i.d. standard normal random variables. Furthermore, in order to approximate the distribution of  $X$  by a lower-dimensional representation in terms of its first principal components, one can replace the smallest diagonal elements of  $D$  by zeros. If applied to a data set instead of a known normal distribution, one first estimates the covariance matrix  $\Sigma$  and then performs a singular value decomposition of the result. The method of PCA thus provides a lower-dimensional

---

\*Corresponding author. Email address: felix.reinbott@ovgu.de

(approximate) representation of a data set, where the chosen principal components can be interpreted as latent factors, and it therefore offers a tool for complexity reduction, i.e. both data compression and pattern detection.

In this article, we are interested in complexity reduction for data of extremes, and care has to be taken when one wants to transfer methods which were designed for the bulk of a data set to its maxima or high-level exceedances. Many classic unsupervised learning procedures have been adapted specifically for this task, see, e.g., [1, 15, 16, 18, 22, 37, 39, 53], and also [26] for a recent overview article. To ensure that an approach is valid for extreme events possibly beyond the observed data, most methods rely on the framework of extreme value theory, which provides additional structure and allows for stability in applications and interpretability of results.

Since the normal distribution is not suitable to describe tails of distributions, the aforementioned motivation of PCA fails when designing a similar approach for extremes. In particular, we want to provide methods for heavy-tailed distributions for which no covariance matrix exists. Furthermore (and this will prove to be a subtle, yet crucial point) extreme value distributions typically live on a restricted set like  $[0, \infty)^d$  which impedes an orthogonal decomposition of its support. Different approaches to solve these two problems have been given by [5, 18, 22, 40], focusing on a suitable transformation of the data and then identifying the linear subspace closest to the data.

We propose a new approach especially suited to the max-stability property of multivariate extreme value distributions that is based on a well-known equivalent formulation of PCA via a regression problem. It allows a transfer from normal to more general distributions and involves in our case techniques from tropical linear algebra, combined with a suitable metric to measure how well the lower dimensional encoding can reconstruct the original data. Tropical linear algebra has proven to be powerful in extremes, see [3] and [28], and tropical variants of PCA also have gained attention for phylogenetic trees, see [61] and [48]. We present several theoretical properties of our approach which motivate its application and aide in interpretation of results. Finally, we present a non-parametric estimator of the optimal projection matrix and show its consistency.

This paper is structured as follows: Section 2 recalls the necessary concepts from extreme value theory, tropical linear algebra and regular PCA. In Section 3 we motivate our definition of PCA for max-stable distributions based on an optimization problem and demonstrate that tropical linear algebra is an appropriate tool to work with max-stable distributions. In Section 4 we investigate properties of the minimizer of our optimization problem, give a complete characterization of distributions that can be mapped down to a lower dimensional space without loss of information in Theorem 1 and show that distributions that are close in some sense to these distributions are also guaranteed to have small reconstruction error. Section 5 outlines a framework for applying max-stable PCA to data, provides a consistency result in Theorem 2 and we demonstrate practical viability with a simulation study and an application to a benchmark dataset.

## 2. Background

### 2.1. Notation and conventions

In the following, we write  $\bigvee_{i=1}^{\infty} x_i := \sup_{i \in \mathbb{N}} x_i$ ,  $\bigvee_{i=1}^d x_i := \max_{i=1}^d x_i$  and  $\bigwedge_{i=1}^{\infty} x_i := \inf_{i \in \mathbb{N}} x_i$ ,  $\bigwedge_{i=1}^d x_i := \min_{i=1}^d x_i$  for  $x_i \in \mathbb{R}$ ,  $i \in \mathbb{N}$ . Vectors are understood as column vectors, with  $x^T, A^T$  denoting the transpose of a vector  $x$  or a matrix  $A$ . Inequalities between vectors are meant componentwise, i.e.  $x \leq y$  for  $x = (x_1, \dots, x_d), y = (y_1, \dots, y_d) \in \mathbb{R}^d$  means that  $x_i \leq y_i$  for all  $i = 1, \dots, d$ , and  $x \not\leq y$  means that there exists an  $i = 1, \dots, d$  such that  $x_i > y_i$ . Accordingly, taking suprema and infima over vectors is done componentwise. The  $d$ -dimensional vectors of all zeros and all ones are denoted by  $\mathbf{0}_d = (0, \dots, 0)$  and  $\mathbf{1}_d = (1, \dots, 1)$ , respectively. Additionally, we denote the  $k$ -th canonical basis vector by  $e_k$ . We write  $\mathbf{0}_{m \times n}$  for an  $m \times n$  all zero matrix and for an  $n \times n$  identity matrix we use the notation  $\text{id}_n$ . We denote the  $i$ -th row of a matrix  $M$  by  $M_i$  and the entry in row  $i$  and column  $j$  of  $M$  by  $M_{ij}$ . The Borel sets on  $\mathbb{R}^d$ , restricted to a Borel set  $A \subseteq \mathbb{R}^d$ , are denoted by  $\mathcal{B}(A)$ . The complement of a set  $A$  is denoted by  $A^c$  and  $\mathbb{1}_A$  denotes the indicator function of  $A$  with  $\mathbb{1}_A(x) = 1$  if  $x \in A$  and 0 if  $x \in A^c$ . The closure of a set  $A$  is denoted by  $\text{cl}(A)$ . We denote a probability space by  $(\Omega, \mathcal{A}, \mathbb{P})$  and the law of some random variable or random vector  $X$  as  $\mathbb{P}^X$ . Equality in distribution, as already mentioned in the introduction, is denoted by  $\stackrel{d}{=}$  and in similar fashion we denote equality almost everywhere by  $\stackrel{a.e.}{=}$ . The Dirac measure in a point  $x$  is denoted by  $\delta_x$ . The space of all non-negative, finitely integrable functions on  $[0, 1]$  is denoted by  $L_+^1([0, 1])$ .

## 2.2. Max-stable distributions

As we are interested in extremal observations of  $d$ -dimensional random vectors we shall subsequently work within the framework of multivariate extreme value theory, see, e.g. [8, 31, 52] for introductions on the topic. To this end, let us consider i.i.d. random vectors  $X_i := (X_{1i}, \dots, X_{di})^T, i \in \mathbb{N}$ , and assume that there exist suitable scaling sequences  $a_n = (a_{1n}, \dots, a_{dn})^T \in (0, \infty)^d, b_n = (b_{1n}, \dots, b_{dn})^T \in \mathbb{R}^d$ , and a distribution function  $G$  such that

$$\mathbb{P}\left(\bigvee_{i=1}^n \frac{X_{1i} - b_{1n}}{a_{1n}} \leq z_1, \dots, \bigvee_{i=1}^n \frac{X_{di} - b_{dn}}{a_{dn}} \leq z_d\right) \rightarrow G(z_1, \dots, z_d), \quad n \rightarrow \infty, \quad (1)$$

holds in all continuity points  $z = (z_1, \dots, z_d)^T \in \mathbb{R}^d$  of  $G$ . If additionally the marginals of  $G$  are non-degenerate, we call  $G$  a multivariate extreme value distribution (MEVD) and by the Fisher-Gnedenko-Tippett theorem it follows that, up to a linear transformation, all marginal distribution functions  $G_1, \dots, G_d$  of  $G$  are of the form

$$G_j(y) = \begin{cases} \exp\left(-(-1 + \gamma_j y)^{-\frac{1}{\gamma_j}}\right), & \gamma_j \neq 0, 1 + \gamma_j y > 0, \\ \exp(-\exp(-y)), & \gamma_j = 0, \\ 0, & \gamma_j > 0, 1 + \gamma_j y \leq 0, \\ 1, & \gamma_j < 0, 1 + \gamma_j y \leq 0, \end{cases}$$

for constants  $\gamma_j \in \mathbb{R}, 1 \leq j \leq d$ , called the extreme value index of the  $j$ th marginal. When the interest is, as in our case, in the extremal dependence structure of a random vector  $X = (X_1, \dots, X_d)^T$ , it is common practise (see, e.g., [31], Section 6.1.2) to first standardize all its marginal distributions. This can be done in a way to ensure convergence of linearly standardized maxima from i.i.d. copies of it to a multivariate extreme value distribution  $G^*$  with identical extreme value indices  $\gamma_j^* = 1, 1 \leq j \leq d$ . In this standardization, we may allow for an arbitrary so-called scale parameter  $\sigma_j > 0$  such that the marginal distribution functions of  $G^*$  satisfy

$$G_j^*(y) = \exp(-\sigma_j/y) \mathbb{1}_{[0, \infty)}(y),$$

where we interpret  $c/0 = \infty$  for  $c > 0$  and  $0/0 = 0$ . We call these marginal distributions 1-Fréchet with scale parameter  $\sigma_j$ . The resulting joint distribution function  $G^*$  has the property that for  $n$  i.i.d. random vectors  $Y_i = (Y_{1i}, \dots, Y_{di})^T, 1 \leq i \leq n$ , with distribution function  $G^*$ , there exist constants  $c_n = (c_{1n}, \dots, c_{dn})^T \in (0, \infty)^d$  such that

$$\left(\bigvee_{i=1}^n \frac{Y_{1i}}{c_{1n}}, \dots, \bigvee_{i=1}^n \frac{Y_{di}}{c_{dn}}\right)^T \stackrel{d}{=} (Y_{11}, \dots, Y_{d1})^T.$$

This is a particularly simple and convenient form (including only a multiplicative standardization) of the property of max-stability, see [32] and [20], and such distributions will be the object of our subsequent analysis.

**Definition 1.** We call a limiting distribution function  $G$  in (1) with marginal distribution functions

$$G_j(y) = \exp(-\sigma_j/y) \mathbb{1}_{[0, \infty)}(y), \quad (2)$$

for  $\sigma_j \geq 0, 1 \leq j \leq d$ , a **max-stable distribution with 1-Fréchet margins**. If a random vector  $X \in [0, \infty)^d$  has such a distribution function  $G$ , then we also call  $X$  **max-stable with 1-Fréchet margins**. If  $\sigma_j > 0$ , then we call the  $j$ th marginal distribution **non-degenerate**.

Note that the use of the term “max-stability” differs in the literature and can also be understood in a more general way (that is including all possible limits in (1) without an assumption about the marginal distributions) or a more restricted one (by assuming that  $\sigma_j = 1, j = 1, \dots, d$ , when one also often speaks of *simple* max-stable distribution). The reason for choosing Definition 1 in our context is that it allows for a unified treatment by fixing the extreme value index of all marginals while at the same time ensuring that max-stable distributions are closed under max-linear transformations, see Lemma 1 below for details, and compare also [20].

In contrast to univariate extreme value distributions, which are essentially determined by their extreme value index (in addition to a location and scale parameter), the class of all multivariate extreme value distributions cannot be

parameterized by a finite set of parameters. Nevertheless, there exist several useful representation results, which we gather below. First, it can be shown (see [51, Proposition 5.11] for the case where  $\sigma_1 = \dots = \sigma_d = 1$  and [38, Corollary 2.7] for the general one) that a distribution function  $G$  is max-stable with 1-Fréchet margins if and only if there exists a bounded measure  $S$  on  $\mathcal{B}(\mathbb{S}_+^{d-1})$  with  $\mathbb{S}_+^{d-1} := \{x \in \mathbb{R}^d : \|x\| = 1\}$  (for some arbitrary but fixed norm  $\|\cdot\|$ ) such that

$$G(z) = \exp\left(-\int_{\mathbb{S}_+^{d-1}} \bigvee_{i=1}^d \frac{a_i}{z_i} S(da)\right) \mathbb{1}_{(0,\infty)^d}(z). \quad (3)$$

The measure  $S$  is called the *spectral measure*. Equivalently, see [30], there exist functions  $f_1, \dots, f_d \in L_+^1([0, 1])$ , called *spectral functions*, such that  $G$  can be written as

$$G(z) = \exp\left(-\int_{[0,1]} \bigvee_{i=1}^d \frac{f_i(e)}{z_i} de\right) \mathbb{1}_{(0,\infty)^d}(z). \quad (4)$$

Note that (2), (3) and (4) imply that, for all  $y > 0$ ,

$$\sigma_j = -y \log(G_j(y)) = \int_{[0,1]} f_j(e) de = \int_{\mathbb{S}_+^{d-1}} a_j S(da), \quad 1 \leq j \leq d. \quad (5)$$

Finally, for our approach to introduce max-stable PCA via a regression problem, we need a way to measure a distance between different components of a max-stable distribution. As [19, 20] and [55] show, a metric for the components of a bivariate max-stable random vector  $(X_1, X_2)$  with spectral functions  $f_1, f_2$  is given by

$$\rho(X_1, X_2) := \int_{[0,1]} |f_1(e) - f_2(e)| de = \|f_1 - f_2\|_1, \quad (6)$$

(which is well-defined even if the choice of  $f_1, f_2$  is not unique, see [19, Section 3] for details) and it metrizes convergence in probability with  $\rho(X_1, X_2) = 0$  implying that  $\mathbb{P}(X_1 = X_2) = 1$ . This metric has been named *spectral distance* in [38]. It can easily be extended to a metric for two random vectors  $X = (X_1, \dots, X_d)^T, Y = (Y_1, \dots, Y_d)^T$  for which  $(X_1, \dots, X_d, Y_1, \dots, Y_d)^T$  is a max-stable random vector by setting

$$\tilde{\rho}(X, Y) := \sum_{k=1}^d \rho(X_k, Y_k). \quad (7)$$

By the above, the metric  $\tilde{\rho}$  metrizes convergence in probability for max-stable random vectors and the statement  $\tilde{\rho}(X, Y) = 0$  is equivalent to  $\mathbb{P}(X = Y) = 1$ . It is thus a suitable metric for measuring how well we can approximate a max-stable random vector by a transformation of it which preserves the max-stability of the random vector but is low-dimensional in a suitable sense. These transformations will be introduced in Section 2.4.

### 2.3. PCA as a regression problem

An alternative motivation for PCA than the one given in the introduction, is the search for an optimal linear subspace of dimension  $p < d$  to project a  $d$ -variate random vector  $X$  upon, where optimality is measured in terms of the second moment of the projection error. It is thus equivalent to finding a solution to the regression problem

$$\min_{(B,W) \in \mathbb{R}^{d \times p} \times \mathbb{R}^{p \times d}} \sum_{k=1}^d \mathbb{E} \left[ (B_k W X - X_k)^2 \right], \quad (8)$$

where  $B_k, 1 \leq k \leq d$ , denotes the  $k$ th row of  $B$ , i.e. in finding an optimal matrix  $W$  which maps our random vector  $X$  to a  $p$ -dimensional subspace and its optimal counterpart  $B$  which reconstructs  $X$  from this lower dimensional representation. If  $E(X_i) = 0, 1 \leq i \leq d$ , and the covariance matrix  $\Sigma := (\text{Cov}(X_i, X_j))_{i,j=1,\dots,d}$  of  $X$  exists, then the orthonormal eigenvectors  $v_1, \dots, v_d$  of  $\Sigma$ , corresponding to the eigenvalues  $\lambda_1 \geq \dots \geq \lambda_d$  can be used to find the optimal matrices as  $B = (v_{ij})_{i=1,\dots,d,j=1,\dots,p}$  and  $W = B^T$ , for a given value of  $p$ . For a proof see [7].

PCA has been adapted to many different settings, see for example [7, 22, 54], and our aim in the following shall be to find an analogue to (8) which is suitable to max-stable random vectors. A first component of this approach has already been found in the metric (7) which shall replace the mean squared distance in (8). Second, we want to make sure that our reconstructed vector is of the same type as the original one. Therefore, in order to stay within the class of max-stable distributions, we replace in (8) the usual matrix product by a max-linear analogue under which max-stable distributions are closed. Details are given in the following subsection.

#### 2.4. Tropical linear algebra and max-stable distributions

If  $X = (X_1, \dots, X_d)^T$  is max-stable with 1-Fréchet margins with distribution function  $G$  according to (3) and (4), respectively, and if  $c_i \geq 0$ ,  $1 \leq i \leq d$ , are constants, then it follows from the above representations that

$$\mathbb{P}\left(\max_{i=1, \dots, d} c_i X_i \leq z\right) = \mathbb{P}(X_i \leq z/c_i, i = 1, \dots, d) = \exp\left(-\frac{1}{z} \int_{[0,1]} \bigvee_{i=1}^d c_i a_i S(da)\right) \mathbb{1}_{[0, \infty)}(z) \quad (9)$$

$$= \exp\left(-\frac{1}{z} \int_{[0,1]} \bigvee_{i=1}^d c_i f_i(e) de\right) \mathbb{1}_{[0, \infty)}(z), \quad z \in \mathbb{R}, \quad (10)$$

see also [29]. Thus, a univariate max-linear combination of the components of a max-stable random vector has a 1-Fréchet-distribution with scale coefficient  $\int_{[0,1]} \bigvee_{i=1}^d c_i f_i(e) de$ . More generally, we can write multiple max-linear combinations of  $X$  given by a matrix  $C \in [0, \infty)^{p \times d}$  conveniently as

$$C \diamond X := \left( \bigvee_{l=1}^d C_{jl} X_l \right)_{j=1, \dots, p}. \quad (11)$$

We will show below in Lemma 1 that the resulting vector has again a max-stable distribution with 1-Fréchet margins. Accordingly, we define a max-linear matrix product by

$$\diamond: [0, \infty)^{d \times p} \times [0, \infty)^{p \times k} \rightarrow [0, \infty)^{d \times k}, \quad (B, W) \mapsto B \diamond W := \left( \bigvee_{l=1}^p B_{il} W_{lj} \right)_{i=1, \dots, d, j=1, \dots, k}. \quad (12)$$

Note that this max-linear matrix product is a bilinear map with respect to the operations  $(\vee, \cdot)$ , where the maximum operation acts as addition, combined with regular scalar multiplication. This framework has been extensively studied in the algebraic literature (often, after a logarithmic transformation, in the isomorphic setting of the operations  $(\vee, +)$ ) under the name tropical linear algebra. For further reading, see the monographs by Butković [13] and by Maclagan and Sturmfels [45] and for related applications of tropical linear algebra to extremes, see, e.g. [3, 11, 28].

### 3. Motivation of max-stable PCA and first properties

We wish to work in the setting of max-stable random vectors and draw some analogies to the Gaussian distribution, which is preserved under linear transformations. This translates directly to max-stable distributions with 1-Fréchet marginals, since they are preserved under max-linear combinations with non-negative scaling factors, as shown in Section 2.4. We will develop a regression approach to PCA based on transformations by tropical linear maps and the metric introduced in (7). But before we do so, we shall first collect a few properties of those max-linear transformations on our random vectors of interest. Our aim is to show that max-linear transformations retain the general structure of max-stable random vectors and that the support of the pushforward measure can easily be characterized.

#### 3.1. Max-linear combinations of max-stable random vectors

We start by taking a closer look at the resulting distribution of the max-linear transformations introduced in Section 2.4, in terms of their spectral measure. Our first lemma below combines the main result from [29] and Proposition 2.6 from [38].

**Lemma 1.** *Let  $X$  be a  $d$ -variate max-stable random vector with non-degenerate 1-Fréchet margins given by a spectral measure  $S$  as in (3). Then for  $H \in [0, \infty)^{p \times d}$ ,  $H \diamond X$  (cf. (11)) is a  $p$ -variate max-stable random vector with 1-Fréchet margins and spectral measure*

$$\tilde{S}(A) = \int_{\{a \in \mathbb{S}_+^{d-1} : \|H \diamond a\| > 0\}} \mathbb{1}_A \left( \frac{H \diamond a}{\|H \diamond a\|} \right) \|H \diamond a\| S(da) \quad \forall A \in \mathcal{B}(\mathbb{S}_+^{p-1}). \quad (13)$$

For the next statement we need to revise some notation. Remember that for a measure  $\mu$  on  $\mathcal{B}(A)$  for some Borel set  $A \subseteq \mathbb{R}^d$ , its support is defined as

$$\text{supp}(\mu) := \{x \in A : \mu(U(x)) > 0, \text{ for all open neighborhoods } U(x) \text{ of } x\}. \quad (14)$$

If  $\mu$  is a finite measure, then an important property we will use later on is that the support is equal to the (well-defined) minimal closed set which has measure  $\mu(A)$ , see [49] II.2, Theorem 2.1. With this definition in mind we give the following proposition, which, up to our knowledge, has not been shown so far but relates to the geometry of max-stable distributions, which was thoroughly investigated in [47].

**Proposition 1.** *Let  $X$  be a  $d$ -variate max-stable random vector with non-degenerate 1-Fréchet margins given by a spectral measure  $S$  as in (3). Then,*

$$\text{supp}(\mathbb{P}^X) = \left\{ \bigvee_{i=1}^d \alpha_i s_i : \alpha_i \geq 0, s_i \in \text{supp}(S) \right\}. \quad (15)$$

For abbreviation, we borrow the notation

$$\vee\text{-span}(\text{supp}(S)) := \left\{ \bigvee_{i=1}^d \alpha_i s_i : \alpha_i \geq 0, s_i \in \text{supp}(S) \right\}$$

(accordingly  $\vee\text{-span}(A)$  is defined for any other subset  $A$  of  $\mathbb{R}^d$  taking the place of  $\text{supp}(S)$ ) from [59] to denote the set on the right hand side of (15). This allows us to characterize the support of a max-stable distribution with 1-Fréchet margins transformed by a max-linear map.

**Corollary 1.** *Let  $X$  be a  $d$ -variate max-stable random vector with non-degenerate 1-Fréchet margins given by a spectral measure  $S$  as in (3). Then for  $H \in [0, \infty)^{p \times d}$ ,  $p \in \mathbb{N}$ , the distribution of the random vector  $H \diamond X$  satisfies*

$$\text{supp}(\mathbb{P}^{H \diamond X}) = \text{cl}(\vee\text{-span}(\{H \diamond s : s \in \text{supp}(S)\})). \quad (16)$$

If  $H$  has no zero columns, then this simplifies to

$$\text{supp}(\mathbb{P}^{H \diamond X}) = \vee\text{-span}(\{H \diamond s : s \in \text{supp}(S)\}). \quad (17)$$

**Remark 1.** The assumption about the non-zero-columns of  $H$  is necessary for (17) to hold as the following example shows: Let  $\|\cdot\| = \|\cdot\|_\infty$  and  $\text{supp}(S) = \{(x, x^2, 1)^T : x \in [0, 1]\}$ . Furthermore, let

$$H = \begin{pmatrix} 1 & 0 & 0 \\ 0 & 1 & 0 \end{pmatrix},$$

thus violating the assumption about no zero columns. Then,

$$(1, 0)^T \notin \{a(x, x^2)^T : a \geq 0, x \in [0, 1]\} = \vee\text{-span}(\{(x, x^2)^T : x \in [0, 1]\}) = \vee\text{-span}(\{H \diamond s : s \in \text{supp}(S)\}),$$

but  $n(1/n, 1/n^2)^T \rightarrow (1, 0)^T$ ,  $n \rightarrow \infty$  and so  $(1, 0)^T \in \text{cl}(\vee\text{-span}(\{H \diamond s : s \in \text{supp}(S)\}))$ .

The previous statements show that the marginal distributions and the general structure of the support of a max-stable random vector  $X$  with 1-Fréchet margins are preserved by max-linear maps. Consequently, they are well suited candidates to map  $X$  to a lower dimensional space.

### 3.2. Definition of max-stable PCA

The aim of this section is to develop a dimension reduction procedure for max-stable distributions that shares many similarities with classic PCA. With the regression approach to PCA from Section 2.3 in mind, we recall that the metric  $\tilde{\rho}$  from (7) measures the distance between two  $d$ -variate max-stable random vectors with 1-Fréchet margins living on the same probability space. We have shown that we can map a  $d$ -variate random vector  $X$  with 1-Fréchet margins to a  $p$ -variate max-stable random vector also with 1-Fréchet margins by using a matrix  $W \in [0, \infty)^{p \times d}$  as follows

$$X \mapsto W \diamond X. \quad (18)$$

We call the mapping (18) an *encoding of  $X$  in  $p$  variables*. If  $p > d$ , by choosing the first  $d$  columns of  $W$  as canonical basis vectors,  $X$  is a subvector of  $W \diamond X$  and the remaining  $p - d$  elements in  $W \diamond X$  add no additional information about  $X$ . Therefore, we will only consider the case  $p \leq d$ . Mapping the encoding back to  $[0, \infty)^d$ , by using a matrix  $B \in [0, \infty)^{d \times p}$  as follows

$$X \mapsto B \diamond W \diamond X, \quad (19)$$

we obtain a  $d$ -variate max-stable random vector with 1-Fréchet margins again. We call (19) a *reconstruction of  $X$  using the matrix  $H = B \diamond W$* . We are interested in encodings and reconstructions of the random vector  $X$  that describe the original distribution of  $X$  as well as possible. In order to measure the quality of the reconstruction, we make use of the semimetric (7) and are ready to define our approach to PCA for max-stable distributions.

**Definition 2.** Let  $X$  be a  $d$ -variate max-stable random vector with 1-Fréchet margins. Then we call a pair of matrices  $(B^*, W^*) \in [0, \infty)^{d \times p} \times [0, \infty)^{p \times d}$  a **max-stable PCA of  $X$  with  $p \leq d$  components**, if it satisfies

$$\tilde{\rho}(B^* \diamond W^* \diamond X, X) = \min_{(B, W) \in [0, \infty)^{d \times p} \times [0, \infty)^{p \times d}} \tilde{\rho}(B \diamond W \diamond X, X). \quad (20)$$

Furthermore, we call the function

$$[0, \infty)^{d \times p} \times [0, \infty)^{p \times d} \rightarrow \mathbb{R}, \quad (B, W) \mapsto \tilde{\rho}(B \diamond W \diamond X, X) \quad (21)$$

the **reconstruction error** of the matrix pair  $(B, W)$  for  $X$ .

**Remark 2.** We want to highlight some key properties of max-stable PCA

1. The construction is a direct adaptation of the regression approach to classic PCA presented in (8), where a distribution is first mapped to a lower dimensional space and then back to the original space using the regular matrix product and the mean squared error distance.
2. Just like regular PCA is particularly suited for data with a Gaussian distribution, since the distribution is preserved under matrix products, our approach preserves the max-stable distribution of the data.
3. The encoding  $W \diamond X$  is an optimal max-linear combination such that we can reconstruct  $X$  as well as possible.
4. We will see below that there always exists a global minimizer of (20). However, it is in general not unique.

In order to solve the minimization problem (20) for a known or estimated distribution of  $X$  we shall first investigate how the reconstruction error depends on the spectral measure of  $X$ .

**Lemma 2.** Let  $X = (X_1, \dots, X_d)^T$  be a  $d$ -variate max-stable random vector with non-degenerate 1-Fréchet margins given by a spectral measure  $S$  as in (3) or spectral functions  $f_1, \dots, f_d \in L_+^1([0, 1])$  as in (4). Then for  $b_i, c_i \geq 0$ ,  $i = 1, \dots, d$ , it holds that

$$\rho \left( \bigvee_{i=1}^d b_i X_i, \bigvee_{i=1}^d c_i X_i \right) = \int_{\mathbb{S}_+^{d-1}} \left| \bigvee_{i=1}^d b_i a_i - \bigvee_{i=1}^d c_i a_i \right| S(da) \quad (22)$$

$$= \int_{[0,1]} \left| \bigvee_{i=1}^d b_i f_i(e) - \bigvee_{i=1}^d c_i f_i(e) \right| de. \quad (23)$$

Using Lemma 2, we can quantify how well a max-stable random vector  $X$  with 1-Fréchet margins is reconstructed by a matrix pair  $(B, W)$  if we know the spectral measure. In particular we can rewrite the reconstruction error (21) from Definition 2 as

$$\tilde{\rho}(B \diamond W \diamond X, X) = \sum_{k=1}^d \rho(B_k \diamond W \diamond X, X_k) = \int_{\mathbb{S}_+^{d-1}} \sum_{k=1}^d |B_k \diamond W \diamond a - a_k| S(da). \quad (24)$$

Because there are consistent estimators of the spectral measure  $S$ , we will use (24) for our statistical analysis of max-stable PCA in Section 5. The next lemma shows that there always exists a max-stable PCA and moreover that it can be found within a compact set that only depends on the dimensions  $d, p$  and the scale parameters of  $X$ .

**Lemma 3.** *Let  $X$  be a  $d$ -variate max-stable random vector with non-degenerate 1-Fréchet margins. Then there exists a constant  $\kappa < \infty$  only depending on  $d, p$  and the marginal scale parameters of  $X$  such that a global minimizer of*

$$(B, W) \mapsto \sum_{k=1}^d \rho(B_k \diamond W \diamond X, X_k) \quad (25)$$

can be found within the compact set

$$K = [0, \kappa]^{d \times p} \times [0, 1]^{p \times d}. \quad (26)$$

#### 4. Properties of max-stable PCA

The properties of a minimizer to (20) differ to properties of classic PCA, due to the fact that we use different operations for the reconstruction matrices and a semimetric which minimizes an absolute value.

Intuition from classic PCA could lead to the conjecture that we can make the choice  $B = W^T$  to half the number of parameters needed. Contrary to intuition, this is *not* the case, as seen by the following example.

**Example 1.** Let  $Z = (Z_1, Z_2)^T$  be a random vector with  $Z_i, i = 1, 2$  i.i.d. 1-Fréchet with scale coefficients equal to one and set

$$A = (A_{ij})_{i=1,2,3,j=1,2} = \begin{pmatrix} 1 & 0 \\ 0 & 1 \\ \frac{1}{2} & \frac{1}{2} \end{pmatrix} \quad (27)$$

to define

$$X := A \diamond Z.$$

Then for all  $x \geq 0$  and  $i = 1, 2, 3$  we have

$$P(X_i \leq x) = P(A_{i1}Z_1 \leq x) \cdot P(A_{i2}Z_2 \leq x) = \exp(-(A_{i1} + A_{i2})/x)$$

and so the random vector  $X$  has 1-Fréchet margins with all marginal scale coefficients equal to one. Now we define

$$H := \begin{pmatrix} 1 & 0 & 0 \\ 0 & 1 & 0 \\ \frac{1}{2} & \frac{1}{2} & 0 \end{pmatrix} = \begin{pmatrix} 1 & 0 \\ 0 & 1 \\ \frac{1}{2} & \frac{1}{2} \end{pmatrix} \diamond \begin{pmatrix} 1 & 0 & 0 \\ 0 & 1 & 0 \end{pmatrix},$$

then it is straightforward to verify

$$H \diamond A = A,$$

and we conclude that for  $p = 2$  there exist matrices  $B, W$  such that the reconstruction error is zero, since it holds that

$$\tilde{\rho}(H \diamond X, X) = \tilde{\rho}(H \diamond A \diamond Z, A \diamond Z) = \tilde{\rho}(A \diamond Z, A \diamond Z) = 0.$$

Now, for a symmetric matrix  $H_s = B \diamond W$  given by  $B, W^T \in [0, \infty)^{3 \times 2}$ , which we assume to satisfy  $\tilde{\rho}(H_s \diamond X, X) = 0$ , to ensure that  $H_s$  also minimizes the distance from reconstruction to the original random vector, we need by Lemma 2 that

$$H_s \diamond A = A. \quad (28)$$



Since  $H_s$  is assumed to be symmetric, we have that  $H_{ij} = H_{ji}$  for all  $i, j = 1, 2, 3$  and equation (28) gives us the following set of equations

$$\begin{aligned} H_{11} \vee \frac{1}{2}H_{13} &= 1, \\ H_{12} \vee \frac{1}{2}H_{13} &= 0, \\ H_{21} \vee \frac{1}{2}H_{23} &= 0, \\ H_{22} \vee \frac{1}{2}H_{23} &= 1, \\ H_{31} \vee \frac{1}{2}H_{33} &= \frac{1}{2}, \\ H_{32} \vee \frac{1}{2}H_{33} &= \frac{1}{2}. \end{aligned}$$

From the second and the third equation and by symmetry of  $H_s$ , it is immediately clear that  $H_{12} = H_{21} = 0$ ,  $H_{13} = H_{31} = 0$  and  $H_{23} = H_{32} = 0$ . This simplifies the set of equations to

$$\begin{aligned} H_{11} &= 1, \\ H_{22} &= 1, \\ H_{33} &= 1. \end{aligned}$$

This means we have only one possible candidate for  $H_s$  given by

$$H_s = \begin{pmatrix} 1 & 0 & 0 \\ 0 & 1 & 0 \\ 0 & 0 & 1 \end{pmatrix}.$$

Since the identity matrix cannot be written as  $B \diamond W$  for any matrices  $B \in [0, \infty)^{3 \times 2}$  and  $W \in [0, \infty)^{2 \times 3}$ , we have a contradiction. This shows that no symmetric matrix can obtain the optimal reconstruction error in this case, therefore symmetric reconstruction matrices are not optimal in general.

In the previous example the max-stable PCA in dimension  $p = 2$  leads to zero reconstruction error because the last row of the matrix  $A$  in (27) is a max-linear combination of the first two rows. We will see in the following that such a structure is characteristic for the cases in which a perfect reconstruction is possible.

In order to study this connection in full generality we need some technical setup and adapt some notation from tropical linear algebra to  $L_+^1([0, 1])$ , facilitating our analysis of spectral functions.

**Definition 3.** If for a family of functions  $f_1, \dots, f_d \in L_+^1([0, 1])$  there exists  $i \in \{1, \dots, d\}$  and constants  $\alpha_j \geq 0$ ,  $j = 1, \dots, d$  such that the following relation holds:

$$f_i \stackrel{a.e.}{=} \bigvee_{j \neq i} \alpha_j f_j,$$

then we call  $f_1, \dots, f_d$   **$\vee$ -linearly dependent**. If  $f_1, \dots, f_d$  are not  $\vee$ -linearly dependent, we call  $f_1, \dots, f_d$   **$\vee$ -linearly independent**.

**Remark 3.** If  $f_1, \dots, f_d \in L_+^1([0, 1])$  are  $\vee$ -linearly independent and there exist coefficients  $\alpha_j \geq 0$ ,  $j = 1, \dots, d$  such that

$$f_1 \stackrel{a.e.}{=} \bigvee_{j=1}^d \alpha_j f_j,$$

then both  $\alpha_1 < 1$  and  $\alpha_1 > 1$  lead to a contradiction to our assumptions and so necessarily  $\alpha_1 = 1$ .

We are interested in the sets obtained by taking finite  $\vee$ -linear combinations of functions from  $L_+^1([0, 1])$  and denote by

$$\vee\text{-span}(\{f_1, \dots, f_d\}) := \left\{ g \in L_+^1([0, 1]) : g \stackrel{\text{a.e.}}{=} \bigvee_{i=1}^d \alpha_i f_i, \alpha_i \geq 0 \right\} \quad (29)$$

the set of functions that coincide with a  $\vee$ -linear combination of  $f_1, \dots, f_d$  almost everywhere.

**Lemma 4.** *Let  $f_1, \dots, f_d, g_1, \dots, g_q \in L_+^1([0, 1])$  with  $q \leq d$  be such that  $g_1, \dots, g_q$  are  $\vee$ -linearly independent and*

$$\vee\text{-span}(f_1, \dots, f_d) = \vee\text{-span}(g_1, \dots, g_q).$$

*Then for each  $j = 1, \dots, q$  there exist  $c_j > 0, i_j \in \{1, \dots, d\}$  such that*

$$g_j \stackrel{\text{a.e.}}{=} c_j f_{i_j}.$$

Lemma 4 tells us that if two families of functions generate the same  $\vee$ -span and one of the families is  $\vee$ -linearly independent, then it is, up to scaling, already contained in the other family. This extends a result from [13], Corollary 3.3.11, to our infinite dimensional setting and is a key argument for our characterization of perfectly reconstructable random vectors. We give a description for class of max-stable distributions that can be reconstructed with zero reconstruction error in the following result.

**Theorem 1.** *Let  $X$  be a  $d$ -variate max-stable random vector with non-degenerate 1-Fréchet margins and let  $p \leq d$ . Then the following statements are equivalent.*

(i) *There exists a pair of matrices  $(B, W) \in [0, \infty)^{d \times p} \times [0, \infty)^{p \times d}$  such that the reconstruction error of the max-stable PCA with  $p$  components satisfies*

$$\tilde{\rho}(B \diamond W \diamond X, X) = 0. \quad (30)$$

(ii) *After possibly permuting the entries of  $X$ , there exists a  $p$ -variate max-stable random vector  $Y$  with non-degenerate 1-Fréchet margins and a matrix  $\Lambda \in [0, \infty)^{(d-p) \times p}$ , such that*

$$X \stackrel{d}{=} \begin{pmatrix} \text{id}_p \\ \Lambda \end{pmatrix} \diamond Y. \quad (31)$$

Furthermore, if (31) holds, we can choose  $(B, W)$  as

$$B = \begin{pmatrix} \text{id}_p \\ \Lambda \end{pmatrix} \quad W = (\text{id}_p, \mathbf{0}_{p \times (d-p)}). \quad (32)$$

We call a random vector  $X$  which satisfies the statements above *perfectly reconstructable* (for a given value of  $p$ ). In essence, this theorem says that a distribution is perfectly reconstructable by max-linear combinations if and only if it has the same distribution as the concatenation of a  $p$ -variate max-stable random vector  $Y$  and  $d - p$  max-linear combinations of  $Y$ .

Note that the matrices  $B$  and  $W$  in (32) contain many zeros, since  $B$  has at least  $p(p - 1)$  and  $W$  has at least  $p(d - 1)$  zero entries, so that there are at least  $p^2 - 2p + dp$  zeros out of  $2dp$  values in total. Furthermore,  $B \diamond W$  also has at least  $(d - p)p + (p - 1)p$  zero entries, yielding that all appearing matrices can be seen as sparse.

In Example 1, we presented a max-linear model that is perfectly reconstructable, given by the matrix (27). It is immediately clear that the matrix (27) has  $p = 2$   $\vee$ -linearly independent rows, since

$$A_3 = \begin{pmatrix} 1 & 1 \\ 2 & 2 \end{pmatrix} = \frac{1}{2}(1, 0) \vee \frac{1}{2}(0, 1) = \frac{1}{2}A_1 \vee \frac{1}{2}A_2.$$

The next result generalizes this observation and entails that perfectly reconstructable distributions with 1-Fréchet margins by max-stable PCA with  $p$  components always have a representation with a matrix that has  $p$   $\vee$ -linear independent rows, yielding a nice analogy to classic PCA.

**Corollary 2.** *Let  $X$  be a  $d$ -variate max-stable random vector with non-degenerate 1-Fréchet margins. Then  $X$  is perfectly reconstructable by max-stable PCA with  $p \leq d$  components (i.e. one of the equivalent statements in Theorem 1 holds), if and only if there exist  $l \in \mathbb{N}$  and an  $l$ -variate max-stable random vector  $Z$  with non-degenerate 1-Fréchet margins and a matrix  $A \in [0, \infty)^{d \times l}$  with at most  $p$   $\vee$ -linearly independent rows such that  $X$  satisfies*

$$X \stackrel{d}{=} A \diamond Z. \quad (33)$$

This result resembles the motivation of classic PCA from the introduction, where PCA perfectly reconstructs a Gaussian random vector  $X$  with  $p$  components, if and only if for  $Z = (Z_1, \dots, Z_p)^T$ ,  $Z_i \stackrel{i.i.d.}{\sim} \mathcal{N}(0, 1)$  and a matrix  $A \in \mathbb{R}^{d \times p}$ ,  $X$  is given by

$$X \stackrel{d}{=} A \cdot Z.$$

Note, however, that in the setting of tropical linear algebra, in contrast to standard linear algebra, there can be more than  $p$   $\vee$ -linearly independent rows in a matrix of dimension  $d \times p$ ,  $p \leq d$ , see, e.g., [13] Theorem 3.4.4. Furthermore, a  $p$ -variate max-stable random vector can in general not be written as a  $\vee$ -max linear combination of  $p$  independent Fréchet random variables: this is only possible if the spectral measure is discrete with  $p$  points of mass and the according models are called max-linear models, see [62] and Section 5.3.1. Accordingly, in the max-stable PCA setting, the latent random vector  $Y$  does not necessarily have independent entries.

## 5. Statistics of max-stable PCA

### 5.1. A consistency result

In this section we outline how to apply max-stable PCA to data. To this end, we should first revisit our assumption of max-stability of all random vectors which appeared in Sections 3 and 4. It was motivated by the fact that max-stable distributions are the only possible limit distributions that can arise for maxima of i.i.d. random vectors with margins standardized to a 1-Fréchet distribution, cf. Section 2.2. This result can in fact be generalized to observations from stationary multivariate time series that satisfy a mild mixing condition, see [8, Theorem 10.22]. Thus, whenever we deal with data that has been obtained by taking maxima from a sufficiently large number of observations we can use a max-stable distribution as an approximation for the resulting multivariate distribution.

Recall that we have used Lemma 2 to obtain a convenient representation of the reconstruction error from Definition 2 by equation (24), namely

$$\tilde{\rho}(B \diamond W \diamond X, X) = \int_{\mathbb{S}_+^{d-1}} \sum_{k=1}^d |B_k \diamond W \diamond a - a_k| S(da).$$

This reformulation of the reconstruction error to be minimized directly lends itself to applications, since there are multiple estimators for the spectral measure, ranging from parametric to nonparametric, and for our purposes, we can use a plugin approach. For different choices to nonparametric estimators see for example [23, 24] and [27, 56, 57] is an incomplete list for semiparametric and parametric alternatives to estimate the spectral measure. We briefly revise a well known non-parametric estimator of the spectral measure  $S$  with good theoretical properties [23]. Let  $X_i = (X_{1i}, \dots, X_{di})^T \in \mathbb{R}^d$  be i.i.d. realizations from a  $d$ -variate distribution function  $F$  with continuous marginals in the max-domain of attraction of a  $d$ -variate extreme value distribution  $G$ . To ensure that we can recover the spectral measure of the transformed limit distribution  $G^*$  with 1-Fréchet margins and equal scale coefficients  $\sigma_1 = \dots = \sigma_d = 1$ , we transform  $X_i$  to a new set of data  $\hat{X}_i^*$  by

$$\hat{X}_{ki}^* = \frac{1}{1 - \hat{F}_k(X_{ki})}, \quad k = 1, \dots, d, \quad (34)$$

where  $\hat{F}_k$  is an estimator of the marginal distribution  $F_k$  obtained from the ranks of the observations given by

$$R_{ki} := \sum_{l=1}^n \mathbb{1}_{\{X_{li} \leq X_{ki}\}}, \quad k = 1, \dots, d, i = 1, \dots, n.$$

Using the ranks  $R_{ki}$ , we set

$$\hat{F}_k(X_{ki}) = \frac{1}{n}(R_{ki} - 1). \quad (35)$$

We do not use the classic empirical distribution function to prevent division by zero in (34). Note that other choices instead of (35) are possible, see [8] (9.37) for example. The transformed data  $\hat{X}_i^*$  can be used to construct a non-parametric estimator for the spectral measure  $S$  on the sphere given by a norm  $\|\cdot\|$  on  $\mathbb{R}^d$  as follows

$$\hat{S}_n(A) := \frac{1}{k} \sum_{i=1}^n \mathbb{1}_{\left\{ \|\hat{X}_i^*\| > \frac{n}{k}, \frac{\hat{X}_i^*}{\|\hat{X}_i^*\|} \in A \right\}}, \quad A \in \mathcal{B}(\mathbb{S}_+^{d-1}). \quad (36)$$

This estimator is based on the "Peaks over threshold" approach, which uses the observations with the largest norms in a data set to estimate extremal characteristics (see, e.g., [8, Section 9.4]). According to this principle, as long as  $k = k(n)$  and  $n$  satisfy suitable growth conditions, it is not necessary for our observations to come from a max-stable distribution. Instead, it is sufficient that they follow a distribution such that i.i.d. observations from this distribution satisfy (1), in order for (36) to be a consistent estimator of the spectral measure for the corresponding max-stable limit. The estimator (36) for the spectral measure has been extensively studied in the literature [8, 23] and is related to many other estimators of the dependence structure (see, e.g., [21, 24, 33]). Thus, using data  $X_1, \dots, X_n$ , instead of the true distribution, we calculate the empirical reconstruction error using the estimated spectral measure, given by

$$\hat{\rho}_n(B \diamond W \diamond X, X) := \int_{\mathbb{S}_+^{d-1}} \sum_{k=1}^d |B_k \diamond W \diamond a - a_k| \hat{S}_n(da). \quad (37)$$

Note that  $\hat{S}_n$  is constructed from the random vectors  $X_1, \dots, X_n$ , therefore it is a random measure. The following general theorem applies to max-stable PCA as a special case, details will be presented later.

**Theorem 2.** *Let  $S$  be a finite measure on  $(\mathbb{S}_+^{d-1}, \mathcal{B}(\mathbb{S}_+^{d-1}))$  and  $(\hat{S}_n)_{n \in \mathbb{N}}$  be a sequence of random finite measures on  $(\mathbb{S}_+^{d-1}, \mathcal{B}(\mathbb{S}_+^{d-1}))$  defined on a common probability space  $(\Omega, \mathcal{A}, \mathbb{P})$ , such that for all continuous functions  $f: \mathbb{S}_+^{d-1} \rightarrow \mathbb{R}$*

$$\int_{\mathbb{S}_+^{d-1}} f(a) \hat{S}_n(da) \xrightarrow{P} \int_{\mathbb{S}_+^{d-1}} f(a) S(da). \quad (38)$$

Furthermore, let  $K \subseteq \mathbb{R}^m$ ,  $m \in \mathbb{N}$  be a compact set and  $c: K \times \mathbb{S}_+^{d-1} \rightarrow \mathbb{R}$  be a continuous function. Then it holds that

(i) *There exists a random sequence  $(\hat{\theta}_n)_{n \in \mathbb{N}} \in K$  on  $(\Omega, \mathcal{A}, \mathbb{P})$  satisfying*

$$\int_{\mathbb{S}_+^{d-1}} c(\hat{\theta}_n, a) \hat{S}_n(da) = \inf_{\theta \in K} \int_{\mathbb{S}_+^{d-1}} c(\theta, a) \hat{S}_n(da) \quad \forall n \in \mathbb{N}. \quad (39)$$

(ii) *For any random sequence  $(\hat{\theta}_n)_{n \in \mathbb{N}}$  satisfying (39), it holds that*

$$\int_{\mathbb{S}_+^{d-1}} c(\hat{\theta}_n, a) S(da) \xrightarrow{P} \inf_{\theta \in K} \int_{\mathbb{S}_+^{d-1}} c(\theta, a) S(da) \quad n \rightarrow \infty. \quad (40)$$

This theorem establishes that for suitable parameter spaces and cost functions, the empirical risk minimization approach does indeed asymptotically minimize the true risk.

**Corollary 3.** *The parameter set*

$$K = [0, \kappa]^{d \times p} \times [0, 1]^{p \times d}$$

from (26) and the cost function

$$c: K \times \mathbb{S}_+^{d-1} \rightarrow \mathbb{R}, \quad (B, W, a) \mapsto \sum_{k=1}^d |B_k \diamond W \diamond a - a_k|,$$

satisfy the conditions of Theorem 2.

*Proof.* Clearly, the given set is compact, and the cost function  $c$  is a continuous function, since it is the composition of continuous functions.  $\square$

For i.i.d. data from a distribution that satisfies (1) (or in other words: that lies in the max-domain of attraction of  $G$ , see [8, Section 8.3]), the estimator (36) converges in the desired sense to the true spectral measure  $S$  of the limit distribution if  $k = k(n) \rightarrow \infty$  and  $\frac{k}{n} \rightarrow 0$ , see [23]. Corollary 3 in combination with Theorem 2 thus shows that asymptotically the true risk is minimized when replacing the unknown  $S$  by the estimator (36) in max-stable PCA.

## 5.2. Implementation

We provide a ready to use implementation of max-stable PCA for the  $R$  programming language at [www.github.com/FelixRb96/maxstablePCA](http://www.github.com/FelixRb96/maxstablePCA), where we find an approximate local minimizer of the reconstruction error using non-linear optimization techniques, since we are not able to analytically compute solutions except for very simple cases. For ease of implementation, we restrict ourselves to the  $l_1$  and  $l_\infty$ -norms, which are both common choices in the "peaks over threshold" approach. We now discuss some properties related to the optimization of the empirical reconstruction error. As a function of  $(B, W)$ , the empirical reconstruction error is generally not convex; however, it is a Lipschitz continuous function that is piecewise linear. Furthermore, note that the following minimization problem yields an upper bound on the minimizer of the empirical reconstruction error

$$\begin{aligned} & \min_{B_{kj}, k=p+1, \dots, d, j=1, \dots, p} \sum_{k=p+1}^d \int_{\mathbb{S}_+^{d-1}} a_k - \bigvee_{j=1}^p B_{kj} a_j \hat{S}_n(da), \\ \text{s.t.} \quad & \max_{k=p+1, \dots, d, j=1, \dots, p, a \in \text{supp}(\hat{S}_n)} B_{kj} a_j \leq a_k, B_{kj} \geq 0. \end{aligned}$$

In the above problem, it can be shown that both the objective function and the constraint function are convex. Therefore, this is a convex optimization problem that provides an upper bound on the optimal empirical reconstruction error.

Even though the function we minimize is not convex, the empirical results presented in the simulation study and data analysis yield good outcomes and encourage the use of our non-linear optimization techniques. We chose to use sequential least squares quadratic programming [41, 44] as our optimization algorithm, despite the reconstruction loss not being differentiable everywhere, because it performed best in simulations compared to other out-of-the-box optimizers available in  $R$ . It converges reasonably fast, and ready-to-use implementations exist.

There are also algorithms with theoretical convergence guarantees to a local minimizer for our problem that could be used instead, see for example [12] or [6]. However, to our knowledge, these alternatives lack fast implementations in  $R$  and depend heavily on good starting values for the problem at hand.

To ensure reasonable results with sequential least squares programming, we uniformly sample a predefined number of points  $(B, W)$  from the set  $[0, 1]^{d \times p} \times [0, 1]^{p \times d}$  and then transform the columns of  $B$  such that  $\|B_{\cdot j}\|_\infty = 1$  for all columns  $j = 1, \dots, p$ . We initialize the optimization algorithm with the sampled value that achieves the smallest empirical reconstruction error. Since the optimization problem is not convex, it is recommended to inspect the result and possibly rerun this procedure multiple times to achieve a good fit. We found that rerunning the simulation studies below with different random seeds will usually lead to the same results up to simultaneous permutations of rows and columns in the result  $(\hat{B}, \hat{W})$ , if enough candidates for starting values are tested.

## 5.3. Simulation study

Since we identified a class of theoretical models that can be perfectly reconstructed by max-stable PCA in Theorem 1 and Corollary 2, and established a consistency result in Theorem 1, it is theoretically justifiable to apply max-stable PCA to data to detect if it approximately follows a distribution as in (31). To demonstrate that the procedure also works in practice, we investigate the finite sample performance of max-stable PCA for simulated data to show behaviors of the procedure that can be expected for real datasets. We propose to plot the empirical reconstruction errors in an "elbow plot" and use a heuristic to choose  $p$  at an "elbow", for the simulated data. Additionally, we recommend plotting the bivariate margins of the data versus the reconstructed data to visually inspect if the reconstruction captures key properties, if the dimension of the data is small. Simulations are carried out using the programming language  $R$  [50] and our  $R$ -package `maxstablePCA`. For reproducibility, the scripts for the simulations are provided in the complementary repository [www.github.com/FelixRb96/maxstablePCA\\_examples](http://www.github.com/FelixRb96/maxstablePCA_examples).

### 5.3.1. Max-linear models

A well studied parametric model for multivariate max-stable distributions are max-linear models [3, 60]. They are popular for evaluating performance of unsupervised learning procedures in multivariate extremes and often appear as model case for these procedures [26, 28, 39]. Max-linear models are  $d$ -variate random vectors  $X$  defined by a latent dimension  $l \in \mathbb{N}$ , a matrix  $A \in [0, \infty)^{d \times l}$  and an  $l$ -variate random vector  $Z$  with  $Z_i, i = 1, \dots, l$ , i.i.d. and  $P(Z_1 \leq x) = \exp(-1/x), x \geq 0$  by setting

$$X := A \diamond Z.$$

By Corollary 2, these models are perfectly reconstructable by max-stable PCA with  $p$  components, if  $A$  is a matrix with  $p$   $\vee$ -linear independent rows. For our simulation, we choose  $l = 3$  and  $d = 5$  by using the matrices

$$A^{(1)} := \begin{pmatrix} \frac{3}{5} & \frac{3}{10} & \frac{1}{10} \\ \frac{1}{20} & \frac{3}{4} & \frac{1}{5} \\ \frac{1}{10} & \frac{1}{10} & \frac{4}{5} \\ \frac{6}{17} & \frac{3}{17} & \frac{8}{17} \\ \frac{1}{3} & \frac{2}{9} & \frac{4}{9} \end{pmatrix}, \quad A^{(2)} := \begin{pmatrix} \frac{2}{3} & 0 & \frac{1}{3} \\ \frac{2}{3} & \frac{1}{3} & 0 \\ 0 & \frac{2}{3} & \frac{1}{3} \\ 0 & \frac{1}{3} & \frac{2}{3} \\ \frac{1}{5} & \frac{3}{5} & \frac{1}{5} \end{pmatrix}. \quad (41)$$

Straightforward calculations show that in the first matrix the first three rows are  $\vee$ -linearly independent and the last two rows are  $\vee$ -linear combinations of the first three rows. Meanwhile, for the second matrix all 5 rows are  $\vee$ -linearly independent. This allows us to shed some light into how the procedure behaves for the two cases of a model that is not perfectly reconstructable and a model that is. We construct two max-linear models  $X^{(i)}$  given by  $Z = (Z_1, Z_2, Z_3)^T$  as above via

$$X^{(i)} := A^{(i)} \diamond Z, \quad i = 1, 2.$$

Now, by Corollary 2,  $X^{(1)}$  is perfectly reconstructable with  $p = 3$ , while  $X^{(2)}$  does not have a representation as in Theorem 1 and therefore is not perfectly reconstructable with  $p \leq 4$ . By our consistency result, we expect that max-stable PCA for the first model should yield a reconstruction error of approximately zero for  $p \geq 3$ , while for the second model the reconstruction error should not vanish for  $p = 1, \dots, 4$ .

We evaluate if we can recover the models well by the empirical procedure. We set up the simulation study by simulating  $n = 10000$  i.i.d. observations of  $X^{(i)}, i = 1, 2$  and use the estimator (36) with  $n/k = 200$ . We let  $p = 1, \dots, 4$  be the number of components in max-stable PCA and plot  $p$  versus the empirical reconstruction error in Figure 1. The plot indicates that at  $p = 3$ , the elbow plot flattens close to zero for the perfectly reconstructable model  $X^{(1)}$  agreeing with our preliminary theoretical considerations up to small approximation errors by the empirical counterparts and optimization errors. For the second model, the elbow plot never reaches zero, indicating that there is a loss of information for all  $p = 1, \dots, 4$ . However, considering the reconstruction for  $p = 3$  for the sample of  $X^{(2)}$  in Figure 2, the max-stable PCA still captures many of the typical rays the max-linear model concentrates around for large values. The estimated matrices  $(\hat{B}, \hat{W})$  for  $p = 3$  are reported in in the Appendix in (B.1) for the perfectly reconstructable case and in (B.2) for the second case. Take note that in both cases, max-stable PCA tends to prioritize one entry of the random vector  $X$  to construct the encoded states  $W \diamond X$ . Also, the matrix used for the reconstruction  $B$  can be seen as close (w.r.t. to the  $\infty$ -norm for example) to a row permuted version of (31) up to rescaling the rows.

### 5.3.2. Logistic models

Since max-linear models are characterized by a discrete spectral measure (see [62]), we will in this section evaluate the performance for max-stable PCA for a spectral measure that allows for a density. The logistic model is one of the most frequently used parametric models for multivariate extreme value theory, see, e.g., [8, Section 9.2.2]. The distribution function of the logistic model with 1-Fréchet margins and all scale coefficients equal to one with parameter  $\beta \in (0, 1]$ , is given by the cumulative distribution function

$$G: \mathbb{R}^d \rightarrow [0, 1], \quad z \mapsto G(z) = \exp \left( - \left( \sum_{k=1}^d \left( \frac{1}{z_k} \right)^{\frac{1}{\beta}} \right)^{\beta} \right) \mathbb{1}_{(0, \infty)^d}(z). \quad (42)$$

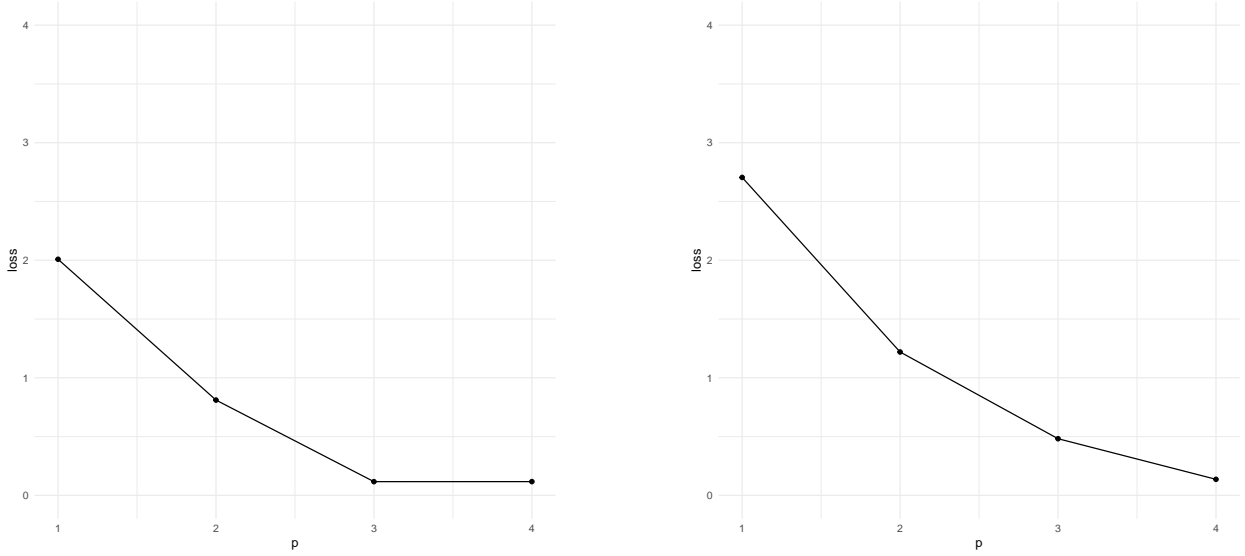


**Fig. 1:** The reconstruction error values of the max-stable PCA for  $p = 1, \dots, 4$  for two max-linear models given by the matrices in (41).

Note that in [17] it has been shown that this distribution function has a spectral density, and the parameter  $\beta$  controls the strength of the dependence between the components. The case  $\beta = 1$  corresponds to complete independence and the limit  $\beta \downarrow 0$  corresponds to full dependence. We simulate from the model with the following three choices for  $\beta$

$$\beta_1 = 0.2, \quad \beta_2 = 0.5, \quad \beta_3 = 0.8.$$

Again, we use the same general setup for our simulation study and sample 10000 i.i.d. observations from the model for the different values of  $\beta$ , set  $\frac{n}{k} = 200$ , fit max-stable PCA to the realizations for  $p = 1, \dots, 4$  and create elbow plots we report in Figure 3, as well as pairplots of the bivariate margins presented in Figure 4. This time for all three models there is no obvious elbow visible. One can therefore conclude that there is no low dimensional factor model that describes the data well in this case. Figure 4 shows the fitted data plotted against the realization in a pairplot for  $p = 3$  and the corresponding estimated matrices are reported in (B.3), (B.4) and (B.5) in the Appendix. Again, in all three cases max-stable PCA tends to highly prioritize one entry of  $X$  to construct each encoded state in  $W \diamond X$  and the matrix  $B$  again is close to (31) up to rescaling and permutation of rows. Note that here the overall values of reconstruction errors decrease the more dependence there is in the data, i.e. the smaller the value of  $\beta$  is. This is not surprising as the limiting  $\beta \downarrow 0$  corresponds to a degenerate model of full dependence, i.e. almost surely equal components, which is perfectly reconstructable even for  $p = 1$ .

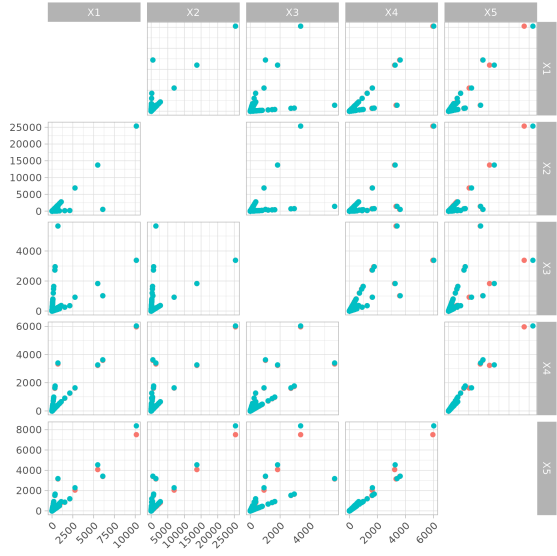
### 5.3.3. A perfectly reconstructable model with latent logistic model

Finally, we simulate from a model where the latent max-stable random vector  $X = A \diamond Z$  is given by a bivariate logistic random vector  $Z = (Z_1, Z_2)^T$  with  $\beta = 0.5$  and a matrix

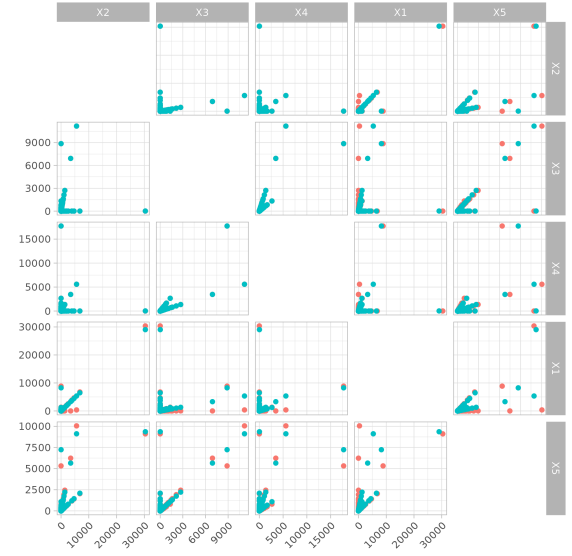
$$A = \begin{pmatrix} \frac{4}{5} & \frac{1}{5} \\ \frac{1}{20} & \frac{19}{20} \\ \frac{3}{5} & \frac{8}{5} \\ \frac{1}{16} & \frac{11}{19} \end{pmatrix}.$$

Again, it can be shown that the conditions of Corollary 2 are met and by defining

$$Y_1 := \frac{4}{5}Z_1 \vee \frac{1}{5}Z_2, \quad Y_2 := \frac{1}{20}Z_1 \vee \frac{19}{20}Z_2$$



(a) Realization of max-linear model with matrix  $A^{(1)}$ . Columns are permuted such that the upper  $3 \times 3$  submatrix is given by the index of the column of the maximal entry in each row of  $\hat{W}$ , as seen in (B.1).



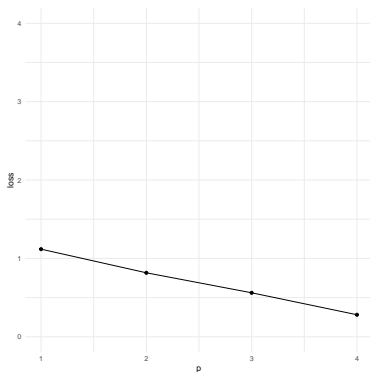
(b) Realization of max-linear model with matrix  $A^{(2)}$ . Columns are permuted such that the upper  $3 \times 3$  submatrix is given by the index of the column of the maximal entry in each row of  $\hat{W}$ , as seen in (B.2).

**Fig. 2:** Pairplots for the two max-linear models. Sample of 10000 i.i.d. realizations (red) of max-linear model with 1-Fréchet margins and all scale coefficients equal to one given by matrix  $A^{(i)}$ ,  $i = 1, 2$ . Plotted against the reconstruction (blue) of max-stable PCA with  $p = 3$ .

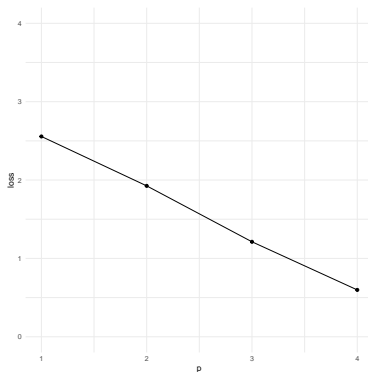
we can write

$$X = \begin{pmatrix} 1 & 0 \\ 0 & 1 \\ 3 & 8 \\ 4 & 19 \\ 9 & 11 \\ 16 & 19 \end{pmatrix} \diamond Y.$$

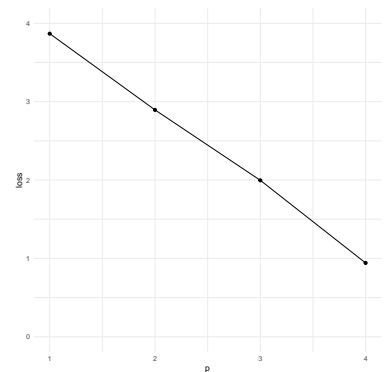
So  $X$  is equal to a model of the form (31) and for  $p = 2$  the theoretical reconstruction error is zero. We again sample  $n = 10000$  i.i.d. realizations of  $X$ , set  $\frac{n}{k} = 200$  for the spectral measure estimator, fit max-stable PCA for  $p = 1, \dots, 4$ , report the reconstruction errors for different values of  $p$  in an elbow plot in Figure 5 and plot the reconstructed data versus the original data in a bivariate margin plot in Figure 5. The elbow plot here again highlights that for  $p = 2$  the empirical error and optimization error are almost zero. It therefore indicates that in this simulation setup, the procedure recovers the theoretical quantities of interest well. We provide the estimated matrices in (B.6) in the Appendix. Again,



(a) Realization of model with  $\beta = 0.2$ .



(b) Realization of model with  $\beta = 0.5$ .



(c) Realization of model with  $\beta = 0.8$ .

**Fig. 3:** The reconstruction error values of the max-stable PCA for  $p = 1, \dots, 4$  for the logistic model with three different values of  $\beta$ .



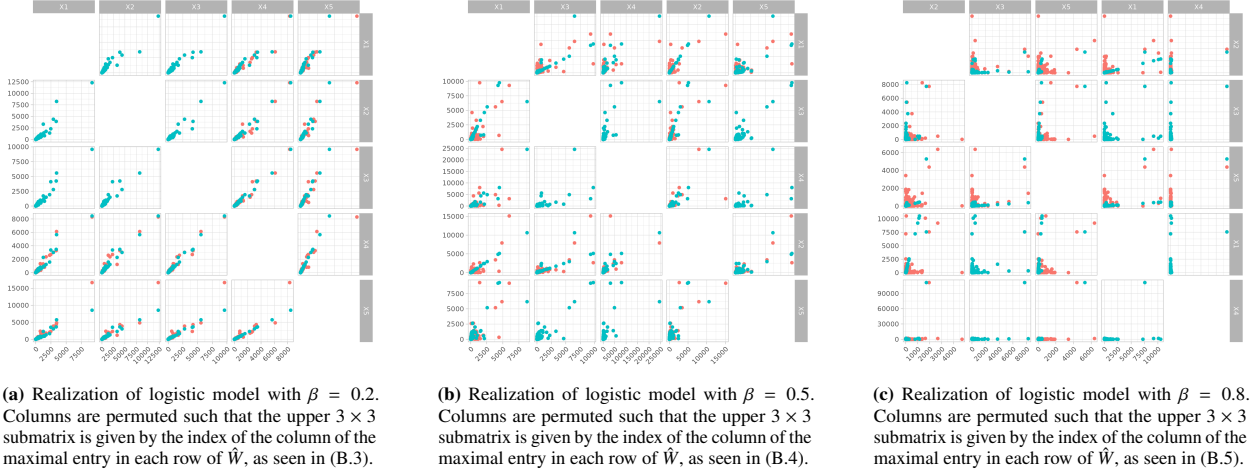


**Fig. 4:** Pairplots for the three logistic models. Sample of 10000 i.i.d. realizations (red) of logistic model with 1-Fréchet margins and all scale coefficients equal to one given by different choices of  $\beta$ . Plotted against the reconstruction (blue) of max-stable PCA with  $p = 3$ .

the largest rowwise entries in  $W$  correspond to the two entries of  $X$  that correspond to the  $\vee$ -linear rows of the matrix  $A$  and  $B$  is close to a matrix as in (31).

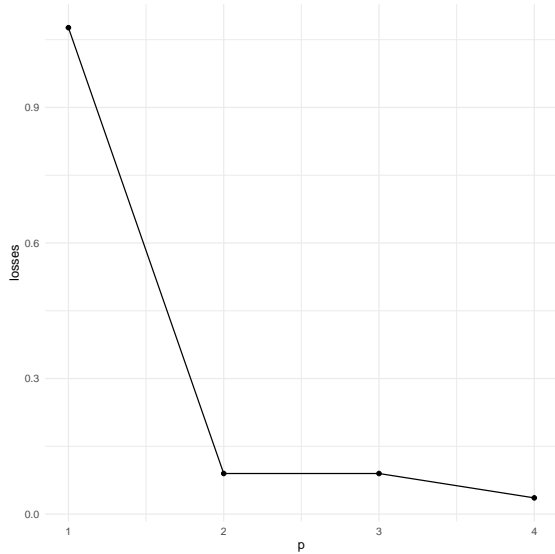
#### 5.4. Danube river data

Finally, we evaluate the performance of max-stable PCA for a real dataset. A ready to use dataset about the Danube river can be found in the R package *graphicalExtremes* [25] and the raw data is available at the website of the Bavarian Environmental agency (<http://www.gkd.bayern.de>). The preprocessed version contains measurements about extreme river discharges of 31 stations in the upper Danube river basin in Bavaria from 1960 to 2009. The data can be seen as stationary, because only the summer months June to August are taken into account, and independent, due to the application of a declustering technique provided by [4]. Therefore, assuming that each row of the data is a realization of an i.i.d. sample is reasonable. This dataset has recently gained a lot of attention in the area of unsupervised learning in extremes, mostly concerned with graphical models [35, 46, 53, 58]. We want to investigate if the distribution of the data transformed to 1-Fréchet margins approximately follows a generalized max-linear factor model, denoted by a random vector  $X$ , given by  $A \in [0, \infty)^{31 \times p}$  with  $p$   $\vee$ -linearly dependent rows and a  $p$  variate random vector  $Z$  with 1-Fréchet margins such that

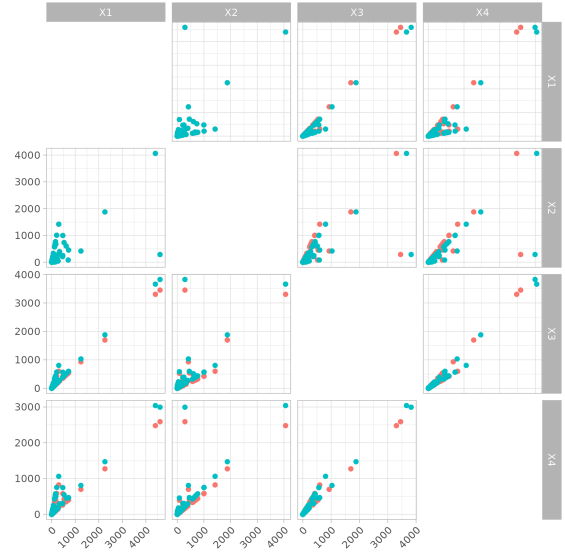
$$X \stackrel{d}{=} A \diamond Z. \quad (43)$$

This model might a priori be a good choice, since the measurement stations are placed on a graph with 6 arms that merge and exploratory data analysis suggests that if we observe an extreme at a measurement station at one arm, it seems highly likely that the adjacent measurement stations will also measure an extreme event. Furthermore, since some river arms are spatially close, there might be a spatial dependence between measurement stations, that might not be fully accounted by the river network structure. The model above can account for the latent spatial dependence between  $p$  components from the river arms in the latent random vector and by virtue of the high dependence in the river arms and their merging, max-linear combinations might be suitable to model the remaining stations. If the reconstruction error for max-stable PCA is small, and we possibly detect an elbow in the elbow plot, we can deduce that the data of the extremes approximately follows such a generalized max-linear factor model.

We perform max-stable PCA for  $p = 1, \dots, 12$  and report the reconstruction losses in an elbow plot for the different values of  $p$  in Figure 6. We use the estimator (36) and since the i.i.d. assumption is reasonable as argued above, the estimator is a suitable choice. For the tuning parameters, we follow the proposed practice by [4, 35, 53], and use the  $l_\infty$ -norm and set the exceedance threshold  $n/k = 10$ , corresponding to a maxima of a row exceeding the  $p = 0.9$  quantile of a standard pareto distribution, yielding 117 observations. In the range of  $p = 4$  to  $p = 8$ , the plot in Fig. 6 flattens out, but without a clear elbow. This is somewhat in line with many analyses [35, 53, 58]. In those works, the authors estimated the graph structure of the data and often reported the best fitting resulting graph to be denser, i.e.



(a) Elbow plot for  $p = 1, \dots, 4$  of the reconstruction error of max-stable PCA for a sample of the model from Section 5.3.3.



(b) Realization of a sample of the model from Section 5.3.3 (red) against the reconstruction by max-stable PCA for  $p = 2$  (blue). Columns are permuted such that the upper  $3 \times 3$  submatrix is given by the index of the column of the maximal entry in each row of  $\hat{W}$ , as seen in (B.6).

**Fig. 5:** Diagnostic plots for applying max-stable PCA to a sample of the generalized max-linear factor model.

more edges, than the flow graph of the river. We further investigate the dataset for max-stable PCA with  $p = 6$ . Since the dimension  $d = 31$  is rather large, instead of the full bivariate margin plot we provide a plot where we take the maxima over each main river arm and compare these maxima taken over the original data and the reconstruction in Figure 10, where we also provide a map of the stations each colored by their corresponding main river arm. We report the loadings for the principal components, that is the rows of the estimated matrix  $W$ , as a heatmap in Figure 7 and provide some further insights into the spatial structure by mapping the rows of  $W$  for  $p = 6$  at the locations of the measurement stations in a map. Additionally, we provide a pairplot of the encoded data  $W \diamond X$  in Figure 7. Figure 8 illustrates the six rows of  $W$  and shows that each of them roughly captures one river arm, where the measurement stations that correspond to a large entry in  $W$  are chosen by the procedure such that they are spatially far from each other. Similarly, we can map the columns of the estimated matrix  $B$  to the measurement stations in Figure 9 to illustrate the generating set of the  $\vee$ -linear space generated by the columns of  $B$ . Note that these columns provide potentially useful insight, since the reconstruction  $B \diamond W \diamond X$  takes values in the  $\vee$ -linear combinations of the columns of  $B$  almost surely. Therefore, these 6 vectors can be seen as the boundary events when only the corresponding entry in  $W \diamond X$  is large. Observe that these columns illustrated in Fig. Figure 9 not only correspond to river arms, but can also show spatial dependence. We conclude that max-stable PCA is a reasonable tool for dimension reduction for this dataset and that further analysis of the encoded state  $W \diamond X$  and the entries of the estimated matrix  $B$  could provide insights into the behavior of extremes for the Danube basin.

## 6. Discussion

In this work, we showed that developing a version of PCA using  $\vee$ -linear combinations and a suitable semimetric for max-stable distributions is a statistically viable procedure that can be used for dimension reduction in multivariate extremes and facilitate a better understanding of high dimensional extreme events.

We discovered that a class of models one might call generalized max-linear factor models given by a matrix  $A \in [0, \infty)^{d \times p}$  and a  $p$ -variate max-stable random vector with 1-Fréchet margins  $Z$  as follows

$$A \diamond Z,$$

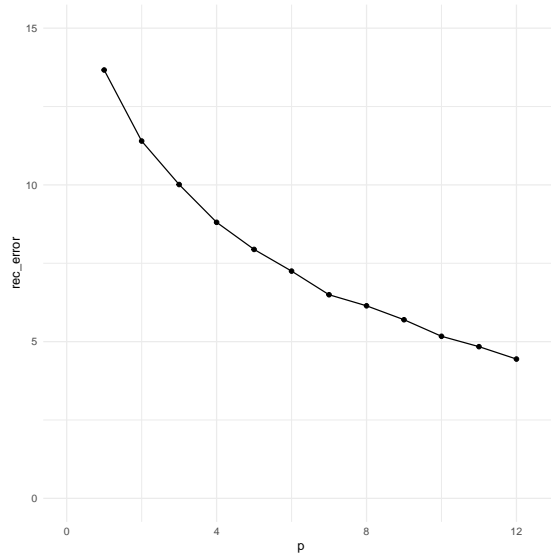


**Fig. 6:** The reconstruction error values of the max-stable PCA for  $p = 1, \dots, 12$ . We used 50 different starting values to find the best reconstruction.

appears as a model case that is perfectly reconstructable, if  $A$  has at most  $p$   $\vee$ -linearly independent rows. This is in analogy to classic PCA, when the data only takes values in a  $p$ -dimensional subspace. Note that since we changed the operation for the matrix, the rows in the matrix  $A$  can potentially all be  $\vee$ -linearly independent even if  $d \gg p$ . This has for example also been recognized in [54] and aligns with the algebraic properties we expect.

We provided a general statement in Theorem 2 that allows to deduce that minimizing some empirical statistical functional of a spectral measure estimator under reasonable assumptions yields an asymptotic minimizer. This statement entails max-stable PCA as a special case but could also be used for other procedures. Finally, we demonstrated that our procedure works well for finite samples in a simulation study and in the analysis of a benchmark dataset.

As an outlook for further work, our theoretical results can also be used to facilitate data analysis of multivariate extreme events with moderate to high asymptotic dependence and provide new insights by providing  $p$  prototypical extreme events that can be seen as building blocks of a good approximation to the data. Additionally, the encoded state can be used as a preprocessing step to reduce the dimension of the data while preserving key features. This might be helpful for applications when fitting a parametric model to the whole dataset of dimension  $d$  is infeasible but fitting it to a  $p$  dimensional model is. Combining this with the matrix  $B$ , it could be used to create a simple procedure to approximately simulate high dimensional extreme events that is easy to interpret.

### Acknowledgements

The authors want to thank Martin Schlather for many helpful discussions that greatly influenced this work and Holger Drees for many helpful comments that improved the quality of the text.

### Funding

Felix Reinbott was funded by the by the Deutsche Forschungsgemeinschaft (DFG, German Research Foundation) - 314838170, GRK 2297 MathCoRe.

### Disclosure Statement

The authors report there are no competing interests to declare.

## Appendix A. Proofs

### Appendix A.1. Proofs of Chapter 3

*Proof of Lemma 1.* The max-linear map defined by  $H$  is continuous, therefore measurable and  $H \diamond X$  is thus a well-defined  $p$ -variate random vector, the distribution function of which we denote by  $\tilde{G}$ . For  $z \in (0, \infty)^p$ , we get from (3) (and with the convention that  $z_i/0 := \infty$  for  $z_i > 0$ ) that

$$\begin{aligned} \tilde{G}(z) &= \mathbb{P} \left( \bigvee_{j=1}^d H_{ij} X_j \leq z_i, i = 1, \dots, p \right) \\ &= \mathbb{P} \left( X_j \leq \frac{z_i}{H_{ij}}, i = 1, \dots, p, j = 1, \dots, d \right) \\ &= \mathbb{P} \left( X_j \leq \bigwedge_{i=1}^p \frac{z_i}{H_{ij}}, j = 1, \dots, d \right) \\ &= \exp \left( - \int_{\mathbb{S}_+^{d-1}} \bigvee_{j=1}^d \bigvee_{i=1}^p \frac{H_{ij} a_j}{z_i} S(da) \right) \\ &= \exp \left( - \int_{\mathbb{S}_+^{d-1}} \bigvee_{i=1}^p \frac{H_i \diamond a}{z_i} S(da) \right). \end{aligned}$$

We can rewrite the expression in the exponent as

$$\begin{aligned} \int_{\mathbb{S}_+^{d-1}} \bigvee_{i=1}^p \frac{H_i \diamond a}{z_i} S(da) &= \int_{\{a \in \mathbb{S}_+^{d-1} : \|H \diamond a\| > 0\}} \bigvee_{i=1}^p \frac{H_i \diamond a}{z_i} S(da) \\ &= \int_{\{a \in \mathbb{S}_+^{d-1} : \|H \diamond a\| > 0\}} \bigvee_{i=1}^p \frac{\frac{H_i \diamond a}{\|H \diamond a\|}}{z_i} \|H \diamond a\| S(da) \\ &= \int_{\mathbb{S}_+^{p-1}} \bigvee_{i=1}^p \frac{\tilde{a}_i}{z_i} \tilde{S}(d\tilde{a}), \end{aligned}$$

where  $\tilde{S}$  is the measure appearing in (13) and the last equality follows by change of variable. Since  $\sup_{a \in \mathbb{S}_+^{d-1}} \|H \diamond a\| < \infty$ , we have furthermore that  $\tilde{S}$  is a finite measure on  $\mathbb{S}_+^{p-1}$ , and therefore a valid spectral measure. This gives us that

$$\tilde{G}(z) = \exp \left( - \int_{\mathbb{S}_+^{p-1}} \bigvee_{i=1}^p \frac{a_i}{z_i} \tilde{S}(da) \right).$$

Clearly, this is the desired form of a max-stable distribution with 1-Fréchet margins.  $\square$

For the proof of Proposition 1 we first recapitulate a useful representation of  $X$  in terms of the points of a Poisson point processes, see [30]. For an introduction to Poisson point processes, see [51], [52] or [43].

**Lemma 5** (cf. Corollary 9.4.5 in [31]). *Let  $X$  be a  $d$ -variate max-stable random vector with non-degenerate 1-Fréchet margins given by a spectral measure  $S$  as in (3). Furthermore, let  $(U_k, A_k)_{k \in \mathbb{N}}$  be a Poisson point process on  $\mathbb{R} \times \mathbb{S}_+^{d-1}$  with intensity measure  $u^{-2} \mathbb{1}_{(0, \infty)}(u) du \times S(da)$ . Then,*

$$X \stackrel{d}{=} \bigvee_{k \in \mathbb{N}} U_k A_k.$$

*Proof.* Let  $N$  denote the random measure associated with  $(U_k, A_k)_{k \in \mathbb{N}}$ , i.e.  $N = \sum_{k=1}^{\infty} \delta_{(U_k, A_k)}$ . Then, for any  $z \in [0, \infty)^d$ , it holds that

$$\begin{aligned}
\mathbb{P}\left(\bigvee_{k \in \mathbb{N}} U_k A_k \leq z\right) &= \mathbb{P}\left(N(\{(u, a) \in (0, \infty) \times \mathbb{S}_+^{d-1} : ua \not\leq z\}) = 0\right) \\
&= \exp\left(-\int_{\mathbb{S}_+^{d-1}} \int_0^{\infty} \frac{1}{u^2} \mathbb{1}_{\{ua \not\leq z\}} du S(da)\right) \\
&= \exp\left(-\int_{\mathbb{S}_+^{d-1}} \int_0^{\infty} \frac{1}{u^2} \mathbb{1}_{\{u > \bigwedge_{i=1}^d \frac{z_i}{a_i}\}} du S(da)\right) \\
&= \exp\left(-\int_{\mathbb{S}_+^{d-1}} \int_{\bigwedge_{i=1}^d \frac{z_i}{a_i}}^{\infty} \frac{1}{u^2} du S(da)\right) \\
&= \exp\left(-\int_{\mathbb{S}_+^{d-1}} \bigvee_{i=1}^d \frac{a_i}{z_i} S(da)\right) \\
&= \mathbb{P}(X \leq z).
\end{aligned}$$

□

*Proof of Proposition 1.* We show (15) by double inclusion.

1.) To show the first inclusion  $\text{supp}(\mathbb{P}^X) \subseteq \vee\text{-span}(\text{supp}(S))$ , use the point process representation of Lemma 5 and note that  $\{U_k, k \in \mathbb{N}\} \subseteq [0, \infty)$  and  $\{A_k, k \in \mathbb{N}\} \subseteq \text{supp}(S)$  almost surely, since  $S((\text{supp}(S))^c) = 0$  by [49] II.2, Theorem 2.1. Additionally, since almost surely only finitely many  $U_k, k \in \mathbb{N}$ , exceed a given positive threshold, at most  $d$  points from  $(U_k, A_k)_{k \in \mathbb{N}}$  suffice to represent the componentwise maximum of  $\bigvee_{k \in \mathbb{N}} U_k A_k$ , yielding  $\bigvee_{k \in \mathbb{N}} U_k A_k \in \vee\text{-span}(\text{supp}(S))$  almost surely. Since  $X \stackrel{d}{=} \bigvee_{k \in \mathbb{N}} U_k A_k$ , we thus get

$$\mathbb{P}^X(\vee\text{-span}(\text{supp}(S))) = \mathbb{P}\left(\bigvee_{k \in \mathbb{N}} U_k A_k \in \vee\text{-span}(\text{supp}(S))\right) = 1.$$

This yields  $\text{supp}(\mathbb{P}^X) \subseteq \vee\text{-span}(\text{supp}(S))$ , by the aforementioned equivalent definition of the support as minimal closed set of full measure, see [49] II.2, Theorem 2.1.

2.) To show the reverse inclusion  $\vee\text{-span}(\text{supp}(S)) \subseteq \text{supp}(\mathbb{P}^X)$ , let first  $x$  be in  $\vee\text{-span}(\text{supp}(S))$ , which implies that there exist  $\alpha_i \geq 0$  and  $s_i \in \text{supp}(S)$ ,  $i = 1, \dots, d$ , such that

$$x = \bigvee_{i=1}^d \alpha_i s_i. \tag{A.1}$$

As long as  $x > \mathbf{0}_d$ , we can choose the above representation in a way such that  $\alpha_i s_i, i = 1, \dots, d$ , are pairwise different, which we will assume in the following. Now, for every open neighborhood  $U(x)$  of  $x$ , there exists an  $\epsilon > 0$  such that the open rectangle  $(x - \epsilon \mathbf{1}_d, x + \epsilon \mathbf{1}_d)$  is contained in  $U(x)$ . Moreover, by simple continuity arguments, there exists a  $\delta > 0$  such that

$$\left(\bigvee_{i=1}^d (\alpha_i - \delta)(s_i - \delta \mathbf{1}_d), \bigvee_{i=1}^d (\alpha_i + \delta)(s_i + \delta \mathbf{1}_d)\right) \subseteq (x - \epsilon \mathbf{1}_d, x + \epsilon \mathbf{1}_d) \subseteq U(x).$$

Define now the sets

$$B_i := (\alpha_i - \delta, \alpha_i + \delta) \times \left((s_i - \delta \mathbf{1}_d, s_i + \delta \mathbf{1}_d) \cap \mathbb{S}_+^{d-1}\right) \subseteq \mathbb{R} \times \mathbb{S}_+^{d-1}$$

for  $i = 1, \dots, d$  and note that by our assumption about the representation (A.1), these sets are pairwise disjoint if  $\delta$  is chosen small enough, which we will again assume in the following.

Next, for the point process representation of  $X$  from Lemma 5, we evaluate the void probabilities of the random measure  $N = \sum_{k=1}^{\infty} \delta_{(U_k, A_k)}$  on the sets  $B_i$ , i.e.  $P(N(B_i) = 0), i = 1, \dots, d$ . We have for each  $i = 1, \dots, d$  that

$$\begin{aligned} & \mathbb{P}(N(B_i) = 0) \\ &= \mathbb{P}\left(N\left((\alpha_i - \delta, \alpha_i + \delta) \times \left((s_i - \delta \mathbf{1}_d, s_i + \delta \mathbf{1}_d) \cap \mathbb{S}_+^{d-1}\right)\right) = 0\right) \\ &= \exp\left(-\int_{0 \vee (\alpha_i - \delta)}^{\alpha_i + \delta} \int_{(s_i - \delta \mathbf{1}_d, s_i + \delta \mathbf{1}_d) \cap \mathbb{S}_+^{d-1}} \frac{1}{u^2} S(da) du\right) \\ &= \exp\left(-S\left((s_i - \delta \mathbf{1}_d, s_i + \delta \mathbf{1}_d) \cap \mathbb{S}_+^{d-1}\right) \int_{0 \vee (\alpha_i - \delta)}^{\alpha_i + \delta} \frac{1}{u^2} du\right). \end{aligned}$$

Since  $s_i \in \text{supp}(S)$ , the set  $(s_i - \delta \mathbf{1}_d, s_i + \delta \mathbf{1}_d) \cap \mathbb{S}_+^{d-1}$  has positive measure with respect to  $S$  and  $(\alpha_i - \delta, \alpha_i + \delta)$  has positive (not necessary finite) measure with respect to  $u^{-2} du$ , hence it holds that  $P(N(B_i) = 0) < 1$  or, equivalently,

$$\mathbb{P}(N(B_i) > 0) > 0, \quad i = 1, \dots, d.$$

Since the sets  $B_i, i = 1, \dots, d$ , were designed to be disjoint, we can conclude from the properties of a Poisson point process that

$$\mathbb{P}(N(B_i) > 0, i = 1, \dots, d) = \prod_{i=1}^d \mathbb{P}(N(B_i) > 0) > 0. \quad (\text{A.2})$$

To conclude our argument, define the exceedance set

$$E(x, \epsilon) := \{(u, a)^T \in \mathbb{R} \times \mathbb{S}_+^{d-1} : ua \not\leq x + \epsilon \mathbf{1}_d\}.$$

Since  $x + \epsilon \mathbf{1}_d > 0$  componentwise, by Lemma 5 it holds that

$$\mathbb{P}(N(E(x, \epsilon)) = 0) = \mathbb{P}\left(\bigvee_{k \in \mathbb{N}} U_k A_k \leq x + \epsilon \mathbf{1}_d\right) = G(x + \epsilon \mathbf{1}_d) > 0. \quad (\text{A.3})$$

Finally, note that

$$\{N(B_i) > 0, i = 1, \dots, d\} \cap \{N(E(x, \epsilon)) = 0\} \subseteq \left\{ \bigvee_{k \in \mathbb{N}} U_k A_k \in U(x) \right\}, \quad (\text{A.4})$$

where the upper interval bound holds due to  $\{N(E(x, \epsilon)) = 0\}$  and the lower interval bound holds by  $\{N(B_i) > 0, i = 1, \dots, d\}$ , see Figure A.11 for an illustration of this fact for  $d = 2$ . Now, since  $B_1, \dots, B_d, E(x, \epsilon)$  are pairwise disjoint and because of (A.2), (A.3) and (A.4), we finally arrive at

$$\begin{aligned} \mathbb{P}^X(U(x)) &= \mathbb{P}\left(\bigvee_{k \in \mathbb{N}} U_k A_k \in U(x)\right) \geq \mathbb{P}(\{N(B_i) > 0, i = 1, \dots, d\} \cap \{N(E(x, \epsilon)) = 0\}) \\ &= \mathbb{P}(N(B_i) > 0, i = 1, \dots, d) \mathbb{P}(N(E(x, \epsilon)) = 0) \\ &> 0. \end{aligned}$$

Thus, each  $x \in \vee\text{-span}(\text{supp}(S)) \cap (0, \infty)^d$  is an element of  $\text{supp}(\mathbb{P}^X)$ . Since the support is a closed set, the same statement follows for all  $x \in \vee\text{-span}(\text{supp}(S))$ , and thus we have shown both inclusions.  $\square$

*Proof of Corollary 1.* It follows from [10], Chapter V, §6 Corollary 4 that

$$\text{supp}(\mathbb{P}^{H \circ X}) = \text{cl}\left(\{H \diamond x : x \in \text{supp}(\mathbb{P}^X)\}\right). \quad (\text{A.5})$$

Proposition 1 gives an explicit representation for  $\text{supp}(\mathbb{P}^X)$ . The bilinearity of  $\diamond$  allows us to rewrite

$$\begin{aligned} \{H \diamond x, x \in \text{supp}(\mathbb{P}^X)\} &= \left\{ H \diamond \bigvee_{i=1}^d \alpha_i s^i : \alpha_i \geq 0, s^i \in \text{supp}(S) \right\} \\ &= \left\{ \bigvee_{i=1}^d \alpha_i (H \diamond s^i) : \alpha_i \geq 0, s^i \in \text{supp}(S) \right\} \\ &= \left\{ \bigvee_{i=1}^p \alpha_i (H \diamond s^i) : \alpha_i \geq 0, s^i \in \text{supp}(S) \right\} \\ &= \vee\text{-span}(\{H \diamond s : s \in \text{supp}(S)\}), \end{aligned} \quad (\text{A.6})$$

where we used in the pen-ultimate equality that  $\bigvee_{i=1}^d \alpha_i (H \diamond s^i)$  can always be represented as a maximum over  $p$  components, since the dimension of this vector is  $p$ . Now, (A.5) and (A.6) give (16).

For the remainder of this proof, we assume that  $H$  has no zero columns. In this case there exists some  $\epsilon > 0$  such that  $\bigvee_{i=1}^p H_{ij} > \epsilon$  for all  $j = 1, \dots, d$  and thus for any  $s = (s_1, \dots, s_d)^T \in \mathbb{S}_+^{d-1}$  it follows that

$$\|H \diamond s\|_\infty = \bigvee_{i=1}^p \bigvee_{j=1}^d H_{ij} s_j = \bigvee_{j=1}^d s_j \bigvee_{i=1}^p H_{ij} \geq \epsilon \bigvee_{j=1}^d s_j = \epsilon \|s\|_\infty.$$

By equivalence of norms there exists some  $c > 0$  such that  $\|s\|_\infty > c$  for all  $s \in \mathbb{S}_+^{d-1}$  and so

$$\|H \diamond s\|_\infty > \epsilon \cdot c > 0$$

for all  $s \in \mathbb{S}_+^{d-1}$ . The set  $\{H \diamond s, s \in \text{supp}(S)\}$  does therefore not include  $\mathbf{0}_d$  and is compact (since  $\text{supp}(S)$  is compact and  $s \mapsto H \diamond s$  is continuous). Thus, by [14] Proposition 25, the set  $\vee\text{-span}(\{H \diamond s, s \in \text{supp}(S)\})$  is closed and the right hand sides of (16) and (17) coincide, which finishes the proof.  $\square$

#### Appendix A.2. Proofs of Chapter 4

*Proof of Lemma 2.* By Lemma 1, the vector  $(Z_1, Z_2)^T := (\bigvee_{i=1}^d b_i X_i, \bigvee_{i=1}^d c_i X_i)^T$  is bivariate max-stable with 1-Fréchet margins. Thus, there exist two spectral functions  $g_1, g_2 \in L_+^1([0, 1])$  such that

$$P(Z_1 \leq z_1, Z_2 \leq z_2) = \exp\left(-\int_{[0,1]} \bigvee_{i=1}^2 \frac{g_i(e)}{z_i} de\right) \mathbb{1}_{[0,\infty)^2}((z_1, z_2)^T)$$

for all  $(z_1, z_2)^T \in \mathbb{R}^2$ . From this we derive that the spectral functions of the max-stable random vector  $(Z_1, Z_2, Z_1 \vee Z_2)^T$  are given by  $g_1, g_2, g_1 \vee g_2 \in L_+^1([0, 1])$ . The definition of  $\rho$  in (6) together with (5) and the fact that

$$x \vee y - x + x \vee y - y = |x - y| \quad (\text{A.7})$$

for all  $x, y \in \mathbb{R}$  then leads to

$$\begin{aligned} \rho(Z_1, Z_2) &= \int_{[0,1]} |g_1(e) - g_2(e)| de = \int_{[0,1]} g_1(e) \vee g_2(e) - g_1(e) + g_1(e) \vee g_2(e) - g_2(e) de \\ &= 2 \int_{[0,1]} g_1(e) \vee g_2(e) de - \int_{[0,1]} g_1(e) de - \int_{[0,1]} g_2(e) de \\ &= 2\sigma_{Z_1 \vee Z_2} - \sigma_{Z_1} - \sigma_{Z_2}, \end{aligned}$$

where  $\sigma_{Z_1 \vee Z_2}$  denotes the scale coefficient of the 1-Fréchet random variable  $Z_1 \vee Z_2$  and  $\sigma_{Z_1}, \sigma_{Z_2}$  denote the scale coefficients of  $Z_1$  and  $Z_2$ , respectively. This allows us to write

$$\rho\left(\bigvee_{i=1}^d b_i X_i, \bigvee_{i=1}^d c_i X_i\right) = 2\sigma_{\bigvee_{i=1}^d b_i X_i \vee c_i X_i} - \sigma_{\bigvee_{i=1}^d b_i X_i} - \sigma_{\bigvee_{i=1}^d c_i X_i}.$$

To show (2), we use the first equation in (5) together with (9) to derive the three scale coefficients and obtain

$$\begin{aligned} \rho\left(\bigvee_{i=1}^d b_i X_i, \bigvee_{i=1}^d c_i X_i\right) &= 2 \int_{\mathbb{S}_+^{d-1}} \bigvee_{i=1}^d (b_i \vee c_i) a_i S(da) - \int_{\mathbb{S}_+^{d-1}} \bigvee_{i=1}^d b_i a_i S(da) - \int_{\mathbb{S}_+^{d-1}} \bigvee_{i=1}^d c_i a_i S(da) \\ &= \int_{\mathbb{S}_+^{d-1}} \left| \bigvee_{i=1}^d b_i a_i - \bigvee_{i=1}^d c_i a_i \right| S(da), \end{aligned}$$

where in the last step we used (A.7) again. The last equality (23) now follows by deriving the scale coefficients using (5) and (10) and calculating by the same arguments as above. We finally arrive at

$$\begin{aligned} \rho\left(\bigvee_{i=1}^d b_i X_i, \bigvee_{i=1}^d c_i X_i\right) &= 2 \int_{\mathbb{S}_+^{d-1}} \bigvee_{i=1}^d (b_i \vee c_i) f_i(e) de - \int_{\mathbb{S}_+^{d-1}} \bigvee_{i=1}^d b_i f_i(e) de - \int_{\mathbb{S}_+^{d-1}} \bigvee_{i=1}^d c_i f_i(e) de \\ &= \int_{\mathbb{S}_+^{d-1}} \left| \bigvee_{i=1}^d b_i f_i(e) - \bigvee_{i=1}^d c_i f_i(e) \right| de. \end{aligned}$$

□

*Proof of Lemma 3.* We split the proof into two parts. First, we derive in (A.12) the value of  $\kappa$  such that for any global minimizer  $(B, W)$ , the largest entry of  $H := B \diamond W$  is bounded by  $\kappa$ . In the second step we show that for any such matrix  $H$ , there exist rescaled matrices  $(\tilde{B}, \tilde{W})$  in the set (26) such that  $H = \tilde{B} \diamond \tilde{W}$ . Together with the continuity of the map (25), this yields the existence of a global minimizer.

1. Let  $(B^*, W^*)$  be a global minimizer of (25) and set  $H^* := B^* \diamond W^*$ . We start by finding an upper bound on  $\tilde{\rho}(H^* \diamond X, X)$  by choosing

$$M := \begin{pmatrix} \text{id}_p \\ \mathbf{0}_{(d-p) \times p} \end{pmatrix} \diamond \begin{pmatrix} \text{id}_p & \mathbf{0}_{p \times (d-p)} \end{pmatrix} = \begin{pmatrix} \text{id}_p & \mathbf{0}_{p \times (d-p)} \\ \mathbf{0}_{(d-p) \times p} & \mathbf{0}_{(d-p) \times (d-p)} \end{pmatrix},$$

Now we use Lemma 2 and (5) to calculate

$$\begin{aligned} \tilde{\rho}(M \diamond X, X) &= \int_{\mathbb{S}_+^{d-1}} \sum_{k=1}^d |M_k \diamond a - a_k| S(da) \\ &= \int_{\mathbb{S}_+^{d-1}} \sum_{k=1}^p |e_k \diamond a - a_k| + \sum_{k=p+1}^d |\mathbf{0}_d \diamond a - a_k| S(da) \\ &= \int_{\mathbb{S}_+^{d-1}} \sum_{k=p+1}^d a_k S(da) \\ &= \sum_{k=p+1}^d \sigma_k. \end{aligned} \tag{A.8}$$

This means that  $\tilde{\rho}(H^* \diamond X, X) \leq \sum_{k=p+1}^d \sigma_k$ . Now let  $i, j \in \{1, \dots, d\}$  be such that  $\|H^*\|_\infty = H_{ij}$ , then

$$\begin{aligned} \tilde{\rho}(H^* \diamond X, X) &= \int_{\mathbb{S}_+^{d-1}} \sum_{k=1}^d |H_k^* \diamond a - a_k| S(da) \\ &\geq \int_{\mathbb{S}_+^{d-1}} |H_i^* \diamond a - a_i| S(da) \\ &\geq \int_{\mathbb{S}_+^{d-1}} H_i^* \diamond a - a_i S(da) \\ &\geq \int_{\mathbb{S}_+^{d-1}} H_{ij}^* a_j - a_i S(da) \\ &= \|H^*\|_\infty \sigma_j - \sigma_i \end{aligned} \tag{A.9}$$



where in the last equality we used again (5). As we assumed  $H^* = B^* \diamond W^*$  for a global minimizer  $(B^*, W^*)$ , we get from (A.8) and (A.9) that

$$\|H^*\|_\infty \sigma_j - \sigma_i \leq \tilde{\rho}(H^* \diamond X, X) \leq \sum_{k=p+1}^d \sigma_k.$$

Since all scale coefficients are positive by assumption, rearranging now gives us the following inequality

$$\|H^*\|_\infty \leq \frac{1}{\sigma_j} \left( \sum_{k=p+1}^d \sigma_k + \sigma_i \right). \quad (\text{A.10})$$

We can now find an upper bound independent of the indices  $i$  and  $j$  by defining  $\sigma_{\min} := \bigwedge_{i=1}^d \sigma_i > 0$  and  $\sigma_{\max} := \bigvee_{i=1}^d \sigma_i$  and the fact that

$$\frac{1}{\sigma_j} \left( \sum_{k=p+1}^d \sigma_k + \sigma_i \right) \leq \frac{1}{\sigma_{\min}} \left( \sum_{k=p+1}^d \sigma_k + \sigma_{\max} \right). \quad (\text{A.11})$$

Setting

$$\kappa := \frac{1}{\sigma_{\min}} \left( \sum_{k=p+1}^d \sigma_k + \sigma_{\max} \right) < \infty, \quad (\text{A.12})$$

and using (A.10) and (A.11), we see that

$$H^* \in [0, \kappa]^{d \times d}. \quad (\text{A.13})$$

for all optimal  $H^* = B^* \diamond W^*$ .

2. For any matrix pair  $(B, W) \in [0, \infty)^{d \times p} \times [0, \infty)^{p \times d}$  and  $H := B \diamond W$ , such that  $\|H\|_\infty \leq \kappa$ , we define a diagonal matrix  $D^{(1)} \in [0, \infty)^{p \times p}$  given by the max-norms of the rows of  $W$  as follows

$$D_{ij}^{(1)} := \begin{cases} \|W_i\|_\infty, & \text{if } i = j, \\ 0, & \text{else.} \end{cases}$$

From this matrix  $D^{(1)}$ , we define another diagonal matrix  $D^{(2)} \in [0, \infty)^{p \times p}$  by

$$D_{ij}^{(2)} := \begin{cases} (D_{ij}^{(1)})^{-1}, & \text{if } i = j, D_{ij}^{(1)} > 0, \\ 0, & \text{else.} \end{cases}$$

Then by construction of the matrices  $D^{(1)}$  and  $D^{(2)}$ , it holds that

$$H = B \diamond W = B \diamond D^{(1)} \diamond D^{(2)} \diamond W. \quad (\text{A.14})$$

Define now  $\tilde{W} := D^{(2)} \diamond W$  and  $\tilde{B} := B \diamond D^{(1)}$  and note that  $\tilde{W} \in [0, 1]^{p \times d}$  and

$$\begin{aligned} \|\tilde{B}\|_\infty &= \|B \diamond D^{(1)}\|_\infty \\ &= \bigvee_{k=1}^d \bigvee_{j=1}^p B_{kj} \|W_j\|_\infty \\ &= \bigvee_{k=1}^d \bigvee_{j=1}^p \bigvee_{l=1}^d B_{kj} W_{jl} \\ &= \|B \diamond W\|_\infty \\ &\leq \kappa, \end{aligned}$$

such that  $\tilde{B} \in [0, \kappa]^{d \times p}$ . Thus, there exists a global minimizer  $(B^*, W^*)$  in  $[0, \kappa]^{d \times p} \times [0, 1]^{p \times d}$ , because the set is compact and the map (25) is continuous.  $\square$

*Proof of Lemma 4.* Because both  $\vee$ -spans of the families  $f_1, \dots, f_d$  and  $g_1, \dots, g_q$  coincide, we have that for each  $g_j$  and  $f_i$ , there exist coefficients  $\Gamma_{ji}, \Lambda_{il} \geq 0$ , such that

$$g_j \stackrel{a.e.}{=} \bigvee_{i=1}^d \Gamma_{ji} f_i, \quad (\text{A.15})$$

$$f_i \stackrel{a.e.}{=} \bigvee_{l=1}^q \Lambda_{il} g_l. \quad (\text{A.16})$$

Let now  $j \in \{1, \dots, q\}$  be fixed and replace the  $f_i$  in (A.15) by the representation of (A.16), so that we obtain

$$g_j \stackrel{a.e.}{=} \bigvee_{i=1}^d \Gamma_{ji} \left( \bigvee_{l=1}^q \Lambda_{il} g_l \right) \stackrel{a.e.}{=} \bigvee_{l=1}^q \left( \bigvee_{i=1}^d \Gamma_{ji} \Lambda_{il} \right) g_l.$$

The  $\vee$ -linear independence of  $g_1, \dots, g_q$  implies by Remark 3 that for every  $j = 1, \dots, q$ , there exists an  $i_j \in \{1, \dots, d\}$  such that  $\Gamma_{ji_j} \Lambda_{i_j j} = 1$  and furthermore the inequality

$$\bigvee_{l \neq j} \left( \bigvee_{i=1}^d \Gamma_{ji} \Lambda_{il} \right) g_l \leq g_j \quad (\text{A.17})$$

holds almost everywhere. This leads to

$$\Gamma_{ji_j} f_{i_j} \stackrel{a.e.}{=} \Gamma_{ji_j} \bigvee_{l=1}^q \Lambda_{i_j l} g_l \stackrel{a.e.}{=} \Gamma_{ji_j} \Lambda_{i_j j} g_j \vee \bigvee_{l \neq j} \Gamma_{ji_j} \Lambda_{i_j l} g_l \stackrel{a.e.}{=} g_j \vee \bigvee_{l \neq j} \Gamma_{ji_j} \Lambda_{i_j l} g_l.$$

In the right hand side of the last expression, the second term is in fact negligible, since  $\Gamma_{ji_j} \Lambda_{i_j l} \leq \bigvee_{i=1}^d \Gamma_{ji} \Lambda_{il}$  and so by (A.17)

$$\bigvee_{l \neq j} \Gamma_{ji_j} \Lambda_{i_j l} g_l \leq \bigvee_{l \neq j} \left( \bigvee_{i=1}^d \Gamma_{ji} \Lambda_{il} \right) g_l \leq g_j.$$

Thus, we have shown that

$$\Gamma_{ji_j} f_{i_j} \stackrel{a.e.}{=} g_j$$

and so the statement follows for  $c_j := \Gamma_{ji_j}$ . Since we have chosen  $\Gamma_{ji_j}$  to satisfy  $\Gamma_{ji_j} \Lambda_{i_j j} = 1$  we can furthermore conclude that  $c_j > 0$ .  $\square$

*Proof of Theorem 1.*

(ii)  $\Rightarrow$  (i) Let (ii) hold and set  $(B, W)$  as in (32). Note that  $W \diamond B = \text{id}_p$ , hence, we obtain

$$B \diamond W \diamond X \stackrel{d}{=} B \diamond W \diamond B \diamond Y = B \diamond Y \stackrel{d}{=} X,$$

which implies

$$\tilde{\rho}(B \diamond W \diamond X, X) = \tilde{\rho}(B \diamond Y, B \diamond Y) = 0.$$

This shows (i) and that  $(B, W)$  in (30) can indeed be chosen as in (32).

(i)  $\Rightarrow$  (ii) Assume that  $(B, W) \in [0, \infty)^{d \times p} \times [0, \infty)^{p \times d}$  exists with  $\tilde{\rho}(B \diamond W \diamond X, X) = 0$  and let  $f = (f_1, \dots, f_d)$  denote a vector of spectral functions from the representation (4) of the distribution function of  $X$ . It follows from  $\tilde{\rho}(B \diamond W \diamond X, X) = 0$  and (23) that

$$\int_{[0,1]} \sum_{k=1}^d |B_k \diamond W \diamond f(e) - f_k(e)| de = 0. \quad (\text{A.18})$$

Hence, the functions  $f_k$  and  $B_k \diamond W \diamond f$  coincide Lebesgue-almost everywhere. Now, define functions

$$g_j: [0, 1] \rightarrow [0, \infty), e \mapsto g_j(e) := W_j \diamond f(e), \quad j = 1, \dots, p.$$

By the definition of  $g_j$  and using (A.18), we get the following two relations

$$\begin{aligned} g_j \in \left\{ \bigvee_{l=1}^d \beta_l f_l : \beta_l \geq 0 \right\} &\subseteq L_+^1([0, 1]), & j = 1, \dots, p, \\ f_i \in \left\{ \bigvee_{j=1}^p \alpha_j g_j : \alpha_j \geq 0 \right\} &\subseteq L_+^1([0, 1]), & i = 1, \dots, d, \end{aligned} \quad (\text{A.19})$$

which implies that

$$\left\{ \bigvee_{l=1}^d \beta_l f_l : \beta_l \geq 0 \right\} = \left\{ \bigvee_{l=1}^d \beta_l \bigvee_{j=1}^p \alpha_{j,l} g_j : \beta_l, \alpha_{j,l} \geq 0 \right\} = \left\{ \bigvee_{j=1}^p \alpha_j g_j : \alpha_j \geq 0 \right\}.$$

In case that the  $p$  functions  $g_1, \dots, g_p$  are not  $\vee$ -linearly independent, we can recursively eliminate functions which can be written as a  $\vee$ -linear combination of the remainders, thereby leading (after suitable reordering of indices) to  $q \leq p$   $\vee$ -linearly independent functions  $g_1, \dots, g_q$  such that

$$\left\{ \bigvee_{j=1}^q \alpha_j g_j : \alpha_j \geq 0 \right\} = \left\{ \bigvee_{j=1}^p \alpha_j g_j : \alpha_j \geq 0 \right\} = \left\{ \bigvee_{l=1}^d \beta_l f_l : \beta_l \geq 0 \right\}. \quad (\text{A.20})$$

Then Lemma 4 applied to the  $\vee$ -linearly independent  $g_1, \dots, g_q$  yields that there exist  $q$  functions among  $f_1, \dots, f_d$  which are rescaled versions of  $g_1, \dots, g_q$ . Apply again a suitable reordering to let this be  $f_1, \dots, f_q$ , so that

$$g_i \stackrel{\text{a.e.}}{=} c_i f_i, \quad i = 1, \dots, q \quad (\text{A.21})$$

for some suitable  $c_i > 0, i = 1, \dots, q$ . Combine (A.19), (A.20) and (A.21) to see that

$$f_i \in \left\{ \bigvee_{l=1}^q \beta_l f_l : \beta_l \geq 0 \right\} = \left\{ \bigvee_{l=1}^p \beta_l f_l : \beta_l \geq 0 \right\}, \quad i = 1, \dots, d.$$

Hence, the  $(d-p)$  spectral functions  $f_{p+1}, \dots, f_d$  are  $\vee$ -linear combinations of  $f_1, \dots, f_p$ . This implies that there exists a matrix  $\Lambda \in [0, \infty)^{(d-p) \times p}$  such that  $f_i \stackrel{\text{a.e.}}{=} \bigvee_{j=1}^p \Lambda_{(i-p),j} f_j, i = p+1, \dots, d$  and we calculate

$$\begin{aligned} \mathbb{P}((X_{p+1}, \dots, X_d)^T \leq z) &= \exp \left( - \int_{[0,1]} \bigvee_{i=p+1}^d \frac{f_i(e)}{z_i} de \right) \mathbb{1}_{[0, \infty)^{d-p}}(z) \\ &= \exp \left( - \int_{[0,1]} \bigvee_{i=p+1}^d \bigvee_{j=1}^p \frac{\Lambda_{(i-p),j} f_j(e)}{z_i} de \right) \mathbb{1}_{[0, \infty)^{d-p}}(z) \\ &= \mathbb{P}(\Lambda \diamond (X_1, \dots, X_p)^T \leq z). \end{aligned}$$

Therefore, the representation of  $(X_{p+1}, \dots, X_d)^T$  by spectral functions is completely determined by the spectral functions of  $X_1, \dots, X_p$  and the matrix  $\Lambda$ . Now set  $Y = (X_1, \dots, X_p)^T$  to achieve (31) and thereby (ii). □

*Proof of Corollary 2.* For the first implication, let  $X$  be perfectly reconstructable. Then by Theorem 1, we have that  $X$ , up to permutation of entries, is in distribution of the form (31). This matrix in (31) has exactly  $p$   $\vee$ -linearly independent rows given by the block matrix  $\text{id}_p$  and (33) holds with this matrix,  $l = p$  and  $Z = Y$ .

For the converse statement, let the distribution of  $X$  be given by (33) and without loss of generality, let the first  $p$  rows of  $A$  be such that they can be used to construct the remaining  $d - p$  rows by  $\vee$ -linear combinations, i.e. there exists a matrix  $\Lambda \in [0, \infty)^{(d-p) \times p}$  such that  $(A_i)_{i=p+1, \dots, d} = \Lambda \diamond (A_i)_{i=1, \dots, p}$ . Next, define a  $p$ -variate random vector  $Y$  by

$$Y_j := X_j = A_j \diamond Z, \quad j = 1, \dots, p.$$

The vector  $Y$  is clearly max-stable with 1-Fréchet margins and for  $X_i, i = p + 1, \dots, d$ , we can write

$$X_i = A_i \diamond Z = \left( \bigvee_{j=1}^p \Lambda_{(i-p), j} A_j \right) \diamond Z = \bigvee_{j=1}^p \Lambda_{(i-p), j} (A_j \diamond Z) = \bigvee_{j=1}^p \Lambda_{(i-p), j} Y_j.$$

Therefore,  $X$  has a representation in distribution given by (31). Theorem 1 thus yields that  $X$  is perfectly reconstructable.  $\square$

### Appendix A.3. Proofs of Chapter 5

*Proof of Theorem 2.* (i) The convergence (38) and the continuity of  $c$  imply that  $\int_{\mathbb{S}_+^{d-1}} c(\theta, a) \hat{S}_n(da)$  is  $\mathcal{A}, \mathbb{B}$ -measurable for each  $\theta \in K, n \in \mathbb{N}$ . Furthermore, for all finite measures  $\mu$  on  $(\mathbb{S}_+^{d-1}, \mathcal{B}(\mathbb{S}_+^{d-1}))$  the function

$$\theta \mapsto \int_{\mathbb{S}_+^{d-1}} c(\theta, a) \mu(da) \tag{A.22}$$

is continuous due to continuity of  $c$ , compactness of  $\mathbb{S}_+^{d-1}$  and since  $\mu$  is finite. The function which maps  $(\omega, \theta) \in \Omega \times K$  to

$$\int_{\mathbb{S}_+^{d-1}} c(\theta, a) \hat{S}_n(da)$$

is thus a Carathéodory function and by the Measurable Maximum Theorem of [2][Theorem 18.19] there exists a random sequence  $(\hat{\theta}_n)_{n \in \mathbb{N}} \in K$  satisfying (39).

(ii) For the second step, note that the function  $(\theta, a) \mapsto c(\theta, a)$  is uniformly continuous on the compact set  $K \times \mathbb{S}_+^{d-1}$ . Thus, for each  $\epsilon > 0$  there exist  $\delta > 0, l \in \mathbb{N}$  and  $\theta_1, \dots, \theta_l \in K$  such that  $B(\theta_i, \delta) := \{\theta \in K : \|\theta - \theta_i\| < \delta\}, i = 1, \dots, l$  is a cover of  $K$  and

$$\sup_{\theta \in B(\theta_i, \delta), a \in \mathbb{S}_+^{d-1}} |c(\theta, a) - c(\theta_i, a)| < \epsilon \tag{A.23}$$

for all  $i = 1, \dots, l$ . Now choose  $\theta \in K$  and let  $i \in \{1, \dots, l\}$  be such that  $\theta \in B(\theta_i, \delta)$ . Then (A.23) yields

$$\begin{aligned} & \left| \int_{\mathbb{S}_+^{d-1}} c(\theta, a) \hat{S}_n(da) - \int_{\mathbb{S}_+^{d-1}} c(\theta, a) S(da) \right| \\ & \leq \left| \int_{\mathbb{S}_+^{d-1}} c(\theta, a) \hat{S}_n(da) - \int_{\mathbb{S}_+^{d-1}} c(\theta_i, a) \hat{S}_n(da) \right| + \left| \int_{\mathbb{S}_+^{d-1}} c(\theta_i, a) \hat{S}_n(da) - \int_{\mathbb{S}_+^{d-1}} c(\theta_i, a) S(da) \right| \\ & + \left| \int_{\mathbb{S}_+^{d-1}} c(\theta_i, a) S(da) - \int_{\mathbb{S}_+^{d-1}} c(\theta, a) S(da) \right| \\ & \leq \epsilon \hat{S}_n(\mathbb{S}_+^{d-1}) + \left| \int_{\mathbb{S}_+^{d-1}} c(\theta_i, a) \hat{S}_n(da) - \int_{\mathbb{S}_+^{d-1}} c(\theta_i, a) S(da) \right| + \epsilon S(\mathbb{S}_+^{d-1}). \end{aligned}$$

Thus,

$$\begin{aligned} & \sup_{\theta \in K} \left| \int_{\mathbb{S}_+^{d-1}} c(\theta, a) \hat{S}_n(da) - \int_{\mathbb{S}_+^{d-1}} c(\theta, a) S(da) \right| \\ & \leq \epsilon (\hat{S}_n(\mathbb{S}_+^{d-1}) + S(\mathbb{S}_+^{d-1})) + \max_{i=1, \dots, l} \left| \int_{\mathbb{S}_+^{d-1}} c(\theta_i, a) \hat{S}_n(da) - \int_{\mathbb{S}_+^{d-1}} c(\theta_i, a) S(da) \right|, \end{aligned}$$

and since the first and the second term converge in probability to  $2\epsilon S(\mathbb{S}_+^{d-1})$  and 0, respectively, by letting  $\epsilon \rightarrow 0$  we conclude

$$\sup_{\theta \in K} \left| \int_{\mathbb{S}_+^{d-1}} c(\theta, a) \hat{S}_n(da) - \int_{\mathbb{S}_+^{d-1}} c(\theta, a) S(da) \right| \xrightarrow{P} 0 \quad (\text{A.24})$$

as  $n \rightarrow \infty$ .

To show now (40), note first that there exists a  $\theta^* \in K$  that satisfies

$$\int_{\mathbb{S}_+^{d-1}} c(\theta^*, a) S(da) = \inf_{\theta \in K} \int_{\mathbb{S}_+^{d-1}} c(\theta, a) S(da)$$

since  $K$  is compact and the function defined in (A.22) (with  $\mu$  replaced by  $S$ ) is continuous. Then for any sequence  $(\hat{\theta}_n)_{n \in \mathbb{N}} \in K$  satisfying (39) we have

$$\begin{aligned} 0 &\leq \int_{\mathbb{S}_+^{d-1}} c(\hat{\theta}_n, a) S(da) - \int_{\mathbb{S}_+^{d-1}} c(\theta^*, a) S(da) \\ &= \int_{\mathbb{S}_+^{d-1}} c(\hat{\theta}_n, a) S(da) - \int_{\mathbb{S}_+^{d-1}} c(\hat{\theta}_n, a) \hat{S}_n(da) + \int_{\mathbb{S}_+^{d-1}} c(\theta^*, a) \hat{S}_n(da) - \int_{\mathbb{S}_+^{d-1}} c(\theta^*, a) S(da) \\ &\quad + \int_{\mathbb{S}_+^{d-1}} c(\hat{\theta}_n, a) \hat{S}_n(da) - \int_{\mathbb{S}_+^{d-1}} c(\theta^*, a) \hat{S}_n(da) \\ &\leq \int_{\mathbb{S}_+^{d-1}} c(\hat{\theta}_n, a) S(da) - \int_{\mathbb{S}_+^{d-1}} c(\hat{\theta}_n, a) \hat{S}_n(da) + \int_{\mathbb{S}_+^{d-1}} c(\theta^*, a) \hat{S}_n(da) - \int_{\mathbb{S}_+^{d-1}} c(\theta^*, a) S(da) =: I + II. \end{aligned}$$

By (A.24) both  $I$  and  $II$  converge to 0 in probability and so the statement follows.  $\square$

## Appendix B. Additional material for the simulation studies

We provide the estimated matrices of the simulation study rounded to two digits for ease of presentation. The estimated matrices of the simulation study with the max-linear models are given by

$$\hat{B}_{mlm}^{(1)} = \begin{pmatrix} 0.07 & 1.31 & 0.45 \\ 0.07 & 0.07 & 1.32 \\ 1.07 & 0.14 & 0.11 \\ 0.64 & 0.78 & 0.08 \\ 0.60 & 0.73 & 0.44 \end{pmatrix}, \quad \hat{W}_{mlm}^{(1)} = \begin{pmatrix} 0.12 & 0.08 & 0.93 & 0.17 & 0.14 \\ 0.77 & 0.18 & 0.01 & 0.10 & 0.05 \\ 0.04 & 0.75 & 0.04 & 0.05 & 0.05 \end{pmatrix} \quad (\text{B.1})$$

$$\hat{B}_{mlm}^{(2)} = \begin{pmatrix} 1.25 & 0.52 & 0.27 \\ 1.31 & 0.00 & 0.00 \\ 0.00 & 0.31 & 1.03 \\ 0.00 & 1.12 & 0.05 \\ 0.40 & 0.32 & 0.84 \end{pmatrix}, \quad \hat{W}_{mlm}^{(2)} = \begin{pmatrix} 0 & 0.76 & 0.00 & 0.00 & 0 \\ 0 & 0.00 & 0.13 & 0.90 & 0 \\ 0 & 0.00 & 0.98 & 0.25 & 0 \end{pmatrix}. \quad (\text{B.2})$$

For the logistic models with  $\beta_1 = 0.2, \beta_2 = 0.5, \beta_3 = 0.8$ , the estimated matrices for  $p = 3$  are given by

$$\hat{B}_{log}^{(1)} = \begin{pmatrix} 0.22 & 0.26 & 1.08 \\ 1.23 & 0.19 & 0.22 \\ 0.27 & 1.02 & 0.20 \\ 0.85 & 0.84 & 0.75 \\ 0.86 & 0.88 & 0.68 \end{pmatrix}, \quad \hat{W}_{log}^{(1)} = \begin{pmatrix} 0.14 & 0.81 & 0.15 & 0.20 & 0.27 \\ 0.13 & 0.19 & 0.98 & 0.26 & 0.41 \\ 0.92 & 0.22 & 0.23 & 0.10 & 0.21 \end{pmatrix} \quad (\text{B.3})$$

$$\hat{B}_{log}^{(2)} = \begin{pmatrix} 0.03 & 0.00 & 1.19 \\ 0.52 & 0.63 & 0.06 \\ 0.06 & 1.20 & 0.01 \\ 1.20 & 0.02 & 0.0 \\ 0.15 & 0.77 & 0.00 \end{pmatrix}, \quad \hat{W}_{log}^{(2)} = \begin{pmatrix} 0.00 & 0.00 & 0.02 & 0.84 & 0.00 \\ 0.00 & 0.03 & 0.83 & 0.02 & 0.03 \\ 0.84 & 0.01 & 0.00 & 0.01 & 0.01 \end{pmatrix} \quad (\text{B.4})$$

$$\hat{B}_{log}^{(3)} = \begin{pmatrix} 0.02 & 0.17 & 0.01 \\ 0.00 & 1.23 & 0.00 \\ 1.43 & 0.00 & 0.00 \\ 0.20 & 0.03 & 0.01 \\ 0.00 & 0.00 & 1.20 \end{pmatrix}, \quad \hat{W}_{log}^{(3)} = \begin{pmatrix} 0 & 0.00 & 0.7 & 0 & 0.00 \\ 0 & 0.81 & 0.0 & 0 & 0.00 \\ 0 & 0.00 & 0.0 & 0 & 0.84 \end{pmatrix}. \quad (\text{B.5})$$

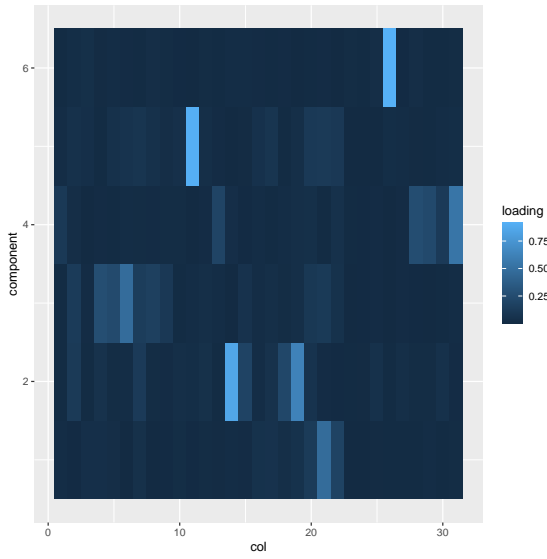
For the simulation of the generalized max-linear model, the estimated matrices are given by

$$\hat{B}_{gen-mlm} = \begin{pmatrix} 1.13 & 0.19 \\ 0.05 & 1.10 \\ 0.94 & 0.62 \\ 0.74 & 0.82 \end{pmatrix}, \quad \hat{W}_{gen-mlm} = \begin{pmatrix} 0.88 & 0.09 & 0.10 & 0.10 \\ 0.02 & 0.91 & 0.04 & 0.07 \end{pmatrix}. \quad (\text{B.6})$$

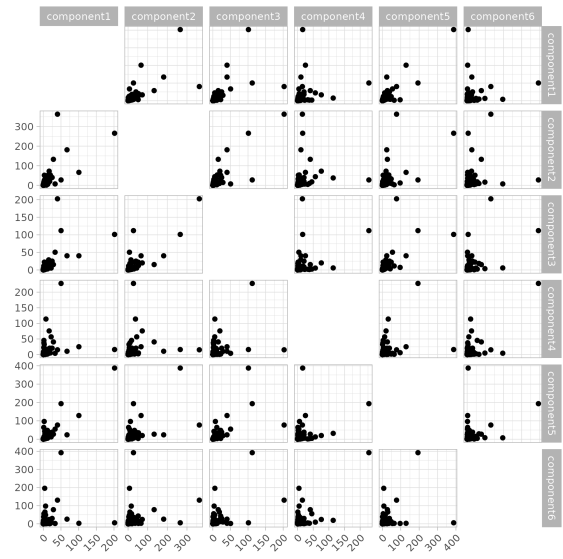
## References

- [1] A. Aghbalou, F. Portier, A. Sabourin, C. Zhou, Tail inverse regression: dimension reduction for prediction of extremes, *Bernoulli* 30 (2024) 503–533.
- [2] C. Aliprantis, K. Border, *Infinite Dimensional Analysis: a Hitchhiker's Guide*, Springer Berlin, Heidelberg, 2006.
- [3] C. Améndola, C. Klüppelberg, S. Lauritzen, N. M. Tran, Conditional independence in max-linear bayesian networks, *The Annals of Applied Probability* 32 (2022) 1 – 45.
- [4] P. Asadi, A. C. Davison, S. Engelke, Extremes on river networks, *The Annals of Applied Statistics* 9 (2015) 2023 – 2050.
- [5] M. Avella-Medina, R. A. Davis, G. Samorodnitsky, Kernel pca for multivariate extremes, arXiv preprint arXiv:2211.13172 (2022).
- [6] A. M. Bagirov, M. Gaudioso, N. Karmitsa, M. M. Mäkelä, S. Taheri, *Numerical nonsmooth optimization*, Springer, 2020.
- [7] P. Baldi, K. Hornik, Neural networks and principal component analysis: Learning from examples without local minima, *Neural networks* 2 (1989) 53–58.
- [8] J. Beirlant, Y. Goegebeur, J. Segers, J. L. Teugels, *Statistics of Extremes: Theory and Applications*, John Wiley & Sons, 2006.
- [9] C. M. Bishop, N. M. Nasrabadi, *Pattern recognition and machine learning*, Springer, 2006.
- [10] N. Bourbaki, *Integration I*, Springer Berlin, 2004.
- [11] J. Buck, C. Klüppelberg, Recursive max-linear models with propagating noise, *Electronic Journal of Statistics* 15 (2021) 4770–4822.
- [12] J. V. Burke, A. S. Lewis, M. L. Overton, A robust gradient sampling algorithm for nonsmooth, nonconvex optimization, *SIAM Journal on Optimization* 15 (2005) 751–779.
- [13] P. Butkovič, *Max-linear Systems: Theory and Algorithms*, Springer Science & Business Media, 2010.
- [14] P. Butkovič, H. Schneider, et al., Generators, extremals and bases of max cones, *Linear algebra and its applications* 421 (2007) 394–406.
- [15] E. Chautru, Dimension reduction in multivariate extreme value analysis, *Electronic Journal of Statistics* 9 (2015) 383–418.
- [16] M. Chiapino, A. Sabourin, Feature clustering for extreme events analysis, with application to extreme stream-flow data, in: *International Workshop on New Frontiers in Mining Complex Patterns*, Springer, pp. 132–147.
- [17] S. G. Coles, J. A. Tawn, Modelling extreme multivariate events, *Journal of the Royal Statistical Society. Series B (Methodological)* 53 (1991) 377–392.
- [18] D. Cooley, E. Thibaud, Decompositions of dependence for high-dimensional extremes, *Biometrika* (2019).
- [19] R. A. Davis, S. I. Resnick, Basic properties and prediction of max-arma processes, *Advances in applied probability* 21 (1989) 781–803.
- [20] R. A. Davis, S. I. Resnick, Prediction of stationary max-stable processes, *The Annals of Applied Probability* 3 (1993) 497 – 525.
- [21] H. Drees, X. Huang, Best attainable rates of convergence for estimators of the stable tail dependence function, *Journal of Multivariate Analysis* 64 (1998) 25–46.
- [22] H. Drees, A. Sabourin, Principal component analysis for multivariate extremes, *Electronic Journal of Statistics* 15 (2021) 908–943.
- [23] J. H. Einmahl, V. I. Piterbarg, L. de Haan, Nonparametric estimation of the spectral measure of an extreme value distribution, *The Annals of Statistics* 29 (2001) 1401–1423.

- [24] J. H. Einmahl, J. Segers, Maximum empirical likelihood estimation of the spectral measure of an extreme-value distribution, *The Annals of Statistics* (2009) 2953–2989.
- [25] S. Engelke, A. S. Hitz, N. Gnecco, M. Hentschel, *graphicalExtremes: Statistical Methodology for Graphical Extreme Value Models*, 2024. R package version 0.3.1.
- [26] S. Engelke, J. Ivanovs, Sparse structures for multivariate extremes, *Annual Review of Statistics and Its Application* 8 (2021) 241–270.
- [27] S. Engelke, A. Malinowski, Z. Kabluchko, M. Schlather, Estimation of hüsler–reiss distributions and brown–resnick processes, *Journal of the Royal Statistical Society: Series B: Statistical Methodology* (2015) 239–265.
- [28] N. Gissibl, C. Klüppelberg, S. Lauritzen, Identifiability and estimation of recursive max-linear models, *Scandinavian Journal of Statistics* 48 (2021) 188–211.
- [29] L. de Haan, A characterization of multidimensional extreme-value distributions, *Sankhyā: The Indian Journal of Statistics, Series A (1961–2002)* 40 (1978) 85–88.
- [30] L. de Haan, A Spectral Representation for Max-stable Processes, *The Annals of Probability* 12 (1984) 1194 – 1204.
- [31] L. de Haan, A. Ferreira, *Extreme Value Theory : An Introduction*, Springer New York, NY, 2006.
- [32] L. de Haan, S. I. Resnick, Limit theory for multivariate sample extremes, *Zeitschrift für Wahrscheinlichkeitstheorie und verwandte Gebiete* 40 (1977) 317–337.
- [33] L. de Haan, S. I. Resnick, Estimating the limit distribution of multivariate extremes, *Stochastic Models* 9 (1993) 275–309.
- [34] T. Hastie, R. Tibshirani, J. H. Friedman, J. H. Friedman, *The elements of statistical learning: data mining, inference, and prediction*, volume 2, Springer, 2009.
- [35] M. Hentschel, S. Engelke, J. Segers, Statistical inference for hüsler-reiss graphical models through matrix completions, *arXiv preprint arXiv:2210.14292* (2022).
- [36] H. Hotelling, Analysis of a complex of statistical variables into principal components., *Journal of educational psychology* 24 (1933) 417.
- [37] H. Jalalzai, R. Leluc, Feature clustering for support identification in extreme regions, in: *International Conference on Machine Learning*, PMLR, pp. 4733–4743.
- [38] A. Janßen, S. Neblung, S. Stoev, Tail-dependence, exceedance sets, and metric embeddings, *Extremes* (2023) 1–39.
- [39] A. Janßen, P. Wan,  $k$ -means clustering of extremes, *Electronic Journal of Statistics* 14 (2020) 1211–1233.
- [40] Y. Jiang, D. Cooley, M. F. Wehner, Principal component analysis for extremes and application to u.s. precipitation, *Journal of Climate* 33 (2020) 6441 – 6451.
- [41] S. G. Johnson, The NLOpt nonlinear-optimization package, <https://github.com/stevengj/nlopt>, 2007.
- [42] I. T. Jolliffe, *Principal Component Analysis*, Springer Series in Statistics, Springer, 2 edition, 2002.
- [43] O. Kallenberg, *Random measures*, De Gruyter, 1983.
- [44] D. Kraft, Algorithm 733: TOMP–fortran modules for optimal control calculations, *ACM Transactions on Mathematical Software* 20 (1994) 262–281.
- [45] D. Maclagan, B. Sturmfels, *Introduction to Tropical Geometry*, volume 161 of Graduate Studies in Mathematics, American Mathematical Society, Providence, RI, 2015.
- [46] L. Mhalla, V. Chavez-Demoulin, D. J. Dupuis, Causal mechanism of extreme river discharges in the upper danube basin network, *Journal of the Royal Statistical Society Series C: Applied Statistics* 69 (2020) 741–764.
- [47] I. Molchanov, Convex geometry of max-stable distributions, *Extremes* 11 (2008) 235–259.
- [48] R. Page, R. Yoshida, L. Zhang, Tropical principal component analysis on the space of phylogenetic trees, *Bioinformatics* 36 (2020) 4590–4598.
- [49] K. R. Parthasarathy, *Probability measures on metric spaces*, Academic Press, New York, 1967.
- [50] R Core Team, *R: A Language and Environment for Statistical Computing*, R Foundation for Statistical Computing, Vienna, Austria, 2024.
- [51] S. I. Resnick, *Extreme Values, Regular Variation and Point Processes*, Springer New York, 1987.
- [52] S. I. Resnick, *Heavy-Tail Phenomena*, Springer New York, 2007.
- [53] F. Röttger, S. Engelke, P. Zwiernik, Total positivity in multivariate extremes, *The Annals of Statistics* 51 (2023) 962–1004.
- [54] M. Schlather, F. Reinbott, A semi-group approach to principal component analysis, 2021.
- [55] S. A. Stoev, M. S. Taqqu, Extremal stochastic integrals: a parallel between max-stable processes and  $\alpha$ -stable processes, *Extremes* 8 (2005) 237–266.
- [56] J. A. Tawn, Bivariate extreme value theory: models and estimation, *Biometrika* 75 (1988) 397–415.
- [57] J. L. Wadsworth, J. A. Tawn, Dependence modelling for spatial extremes, *Biometrika* 99 (2012) 253–272.
- [58] P. Wan, C. Zhou, Graphical lasso for extremes, *arXiv preprint arXiv:2307.15004* (2023).
- [59] Y. Wang, S. A. Stoev, On the structure and representations of max-stable processes, *Advances in Applied Probability* 42 (2010) 855–877.
- [60] Y. Wang, S. A. Stoev, Conditional sampling for spectrally discrete max-stable random fields, *Advances in Applied Probability* 43 (2011) 461–483.
- [61] R. Yoshida, L. Zhang, X. Zhang, Tropical principal component analysis and its application to phylogenetics, *Bulletin of mathematical biology* 81 (2019) 568–597.
- [62] R. Yuen, S. Stoev, CRPS M-estimation for max-stable models, *Extremes* 17 (2014) 387–410.



(a) The estimated matrix  $W$  plotted as a heatmap. Each entry is a tile in the plot, and the lighter the blue color, the larger the entry in  $W$ .



(b) The data transformed to 1-Fréchet scale and then we applied the matrix  $W$  to plot the bivariate margins of the 6 entries of  $W \diamond X$ .

**Fig. 7:** Diagnostic plots about the encoded data  $W \diamond X$  on 1-Fréchet margins.

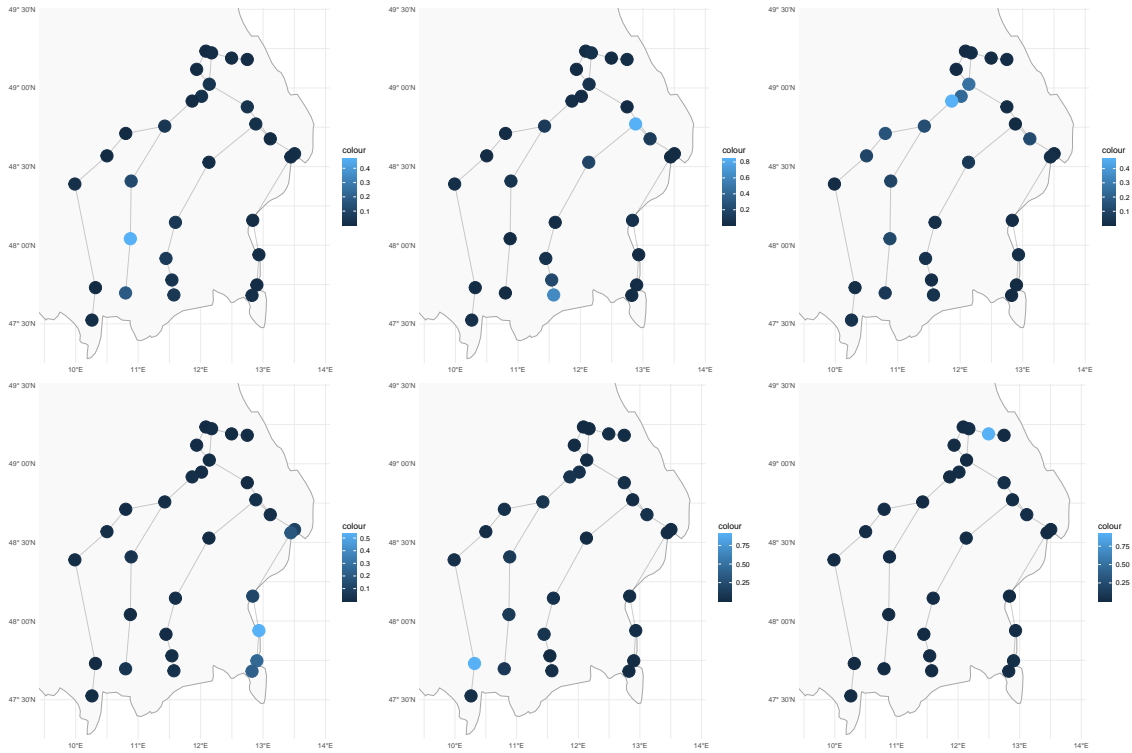


**Fig. 8:** The rows of the estimated  $W$  for  $p = 6$  mapped to their spatial locations ( $W_{ji}$  corresponds to station  $i$  and component  $j$ ), where the largest entry  $W_{ji}$  has the lightest blue color. The top row contains the first three rows and the second row the last three. Observe that each encoded state highly loads stations from the same riverarm. This holds true also for the upper middle plot, see Figure 10.



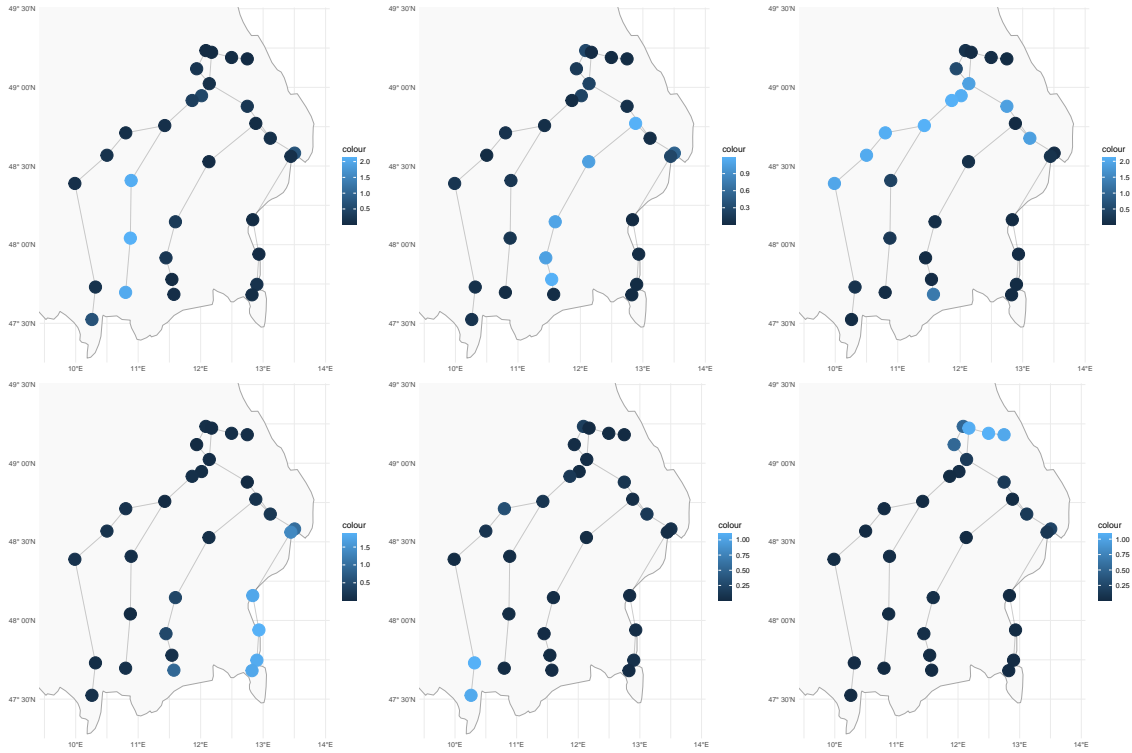


**Fig. 9:** The columns of the estimated  $B$  for  $p = 6$  mapped to their spatial locations ( $B_{ij}$  corresponds to station  $i$  and encoded state  $j$ ) and colored by the entry in  $B$ , where a larger  $B_{ij}$  has a lighter blue color. The top row contains the first three columns and the second row the last three. Note that high values in a column  $j$  of  $B$  appear on the same riverarm as the point with the highest value in row  $j$  of the matrix  $W$ , compare with Figure 8.

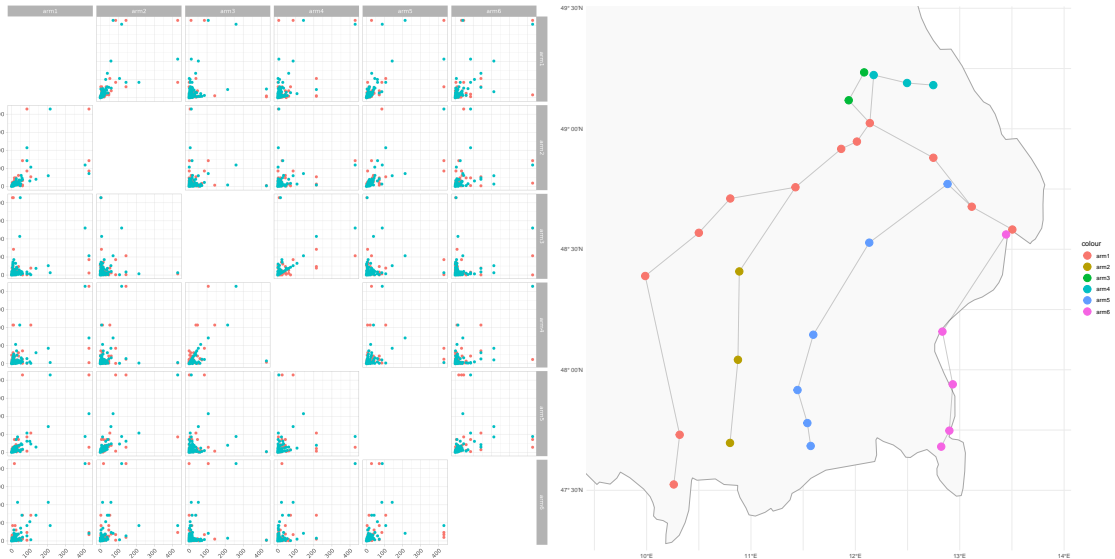


**Fig. 10:** On the left: Data of the maxima over each river arm (red) versus the maxima of each river arm of the reconstruction by max-stable PCA for  $p = 6$ , both on 1-Fréchet scale. On the right: The stations colored by the river arm they belong to. Note that this is only the river network of stations appearing and other inflows are not taken into account.

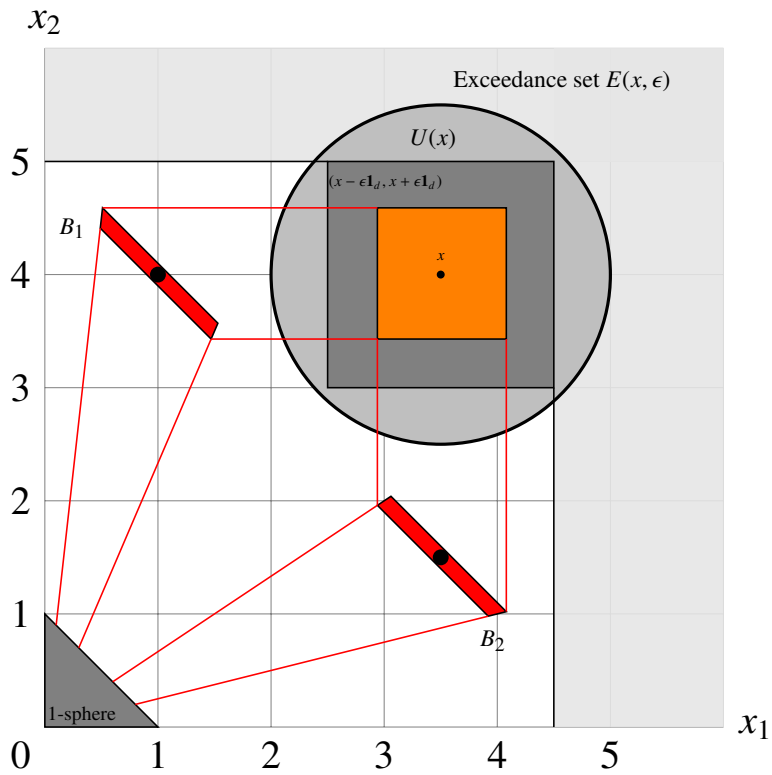


**Fig. A.11:** A visualization of the sets appearing in the proof for  $d = 2$  and  $x = (3.5, 4)$  in Cartesian coordinates. The neighbourhood  $U(x)$  is given by a circle of radius  $r = 1.5$  around  $x$  and  $\epsilon = 1$  defines the dark grey rectangle  $(x - \epsilon \mathbf{1}_2, x + \epsilon \mathbf{1}_2)$ . Let  $s_1 = (\frac{7}{10}, \frac{3}{10})$ ,  $s_2 = (\frac{1}{5}, \frac{4}{5})$ , then we write  $x = \alpha_1 s_1 \vee \alpha_2 s_2$  with  $\alpha_1 = \alpha_2 = 5$  and setting  $\delta = \frac{1}{10}$  yields the sets  $B_1$  and  $B_2$ , where the graphic shows the preimage of those sets under the polar coordinate transform. The orange set contains all coordinatewise maxima of one point from the set  $B_1$  and one point from the set  $B_2$ . The exceedance set  $E(x, \epsilon)$  is the light grey L shaped set.